Article

Syntheses and Properties of Two-Dimensional Charged Nonlinear Optical Chromophores Incorporating Redox-Switchable *cis*-Tetraammineruthenium(II) Centers

Benjamin J. Coe, James A. Harris, Lathe A. Jones, Bruce S. Brunschwig, Kai Song, Koen Clays, Javier Garn, Jess Orduna, Simon J. Coles, and Michael B. Hursthouse

J. Am. Chem. Soc., **2005**, 127 (13), 4845-4859• DOI: 10.1021/ja0424124 • Publication Date (Web): 10 March 2005

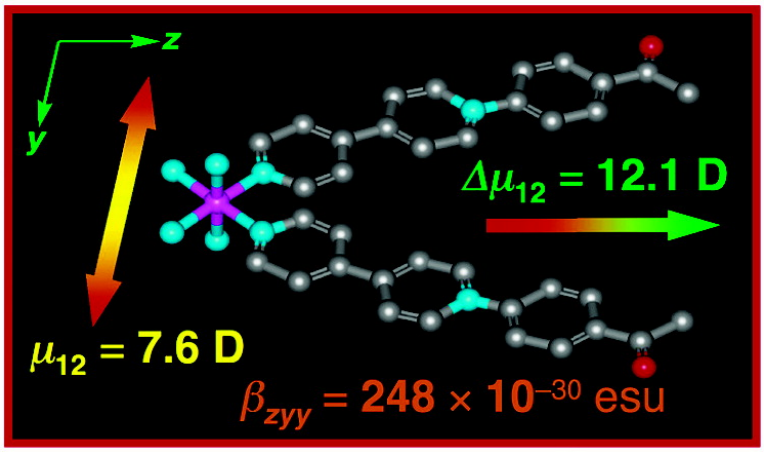

More About This Article

Additional resources and features associated with this article are available within the HTML version:

- Supporting Information
- Links to the 10 articles that cite this article, as of the time of this article download
- Access to high resolution figures
- Links to articles and content related to this article
- Copyright permission to reproduce figures and/or text from this article

View the Full Text HTML

J|A|C|S
ARTICLES
Published on Web 03/10/2005

Syntheses and Properties of Two-Dimensional Charged Nonlinear Optical Chromophores Incorporating Redox-Switchable *cis*-Tetraammineruthenium(II) Centers

Benjamin J. Coe,*[,†] James A. Harris,[†,⊥] Lathe A. Jones,[†] Bruce S. Brunschwig,[‡,⊥] Kai Song,[§] Koen Clays,[§] Javier Garín,[||] Jesús Orduna,[||] Simon J. Coles,[#] and Michael B. Hursthouse[#]

Contribution from the School of Chemistry, University of Manchester, Oxford Road, Manchester, U.K. M13 9PL, Chemistry Department, Brookhaven National Laboratory, P.O. Box 5000, Upton, New York 11973-5000, Laboratory of Chemical and Biological Dynamics, Center for Research on Molecular Electronics and Photonics, University of Leuven, Celestijnenlaan 200D, B-3001 Leuven, Belgium, Departamento de Química Orgánica, ICMA, Universidad de Zaragoza-CSIC, E-50009 Zaragoza, Spain, and EPSRC National Crystallography Service, School of Chemistry, University of Southampton, Highfield, Southampton, U.K. SO17 1BJ

Received December 17, 2004; E-mail: b.coe@man.ac.uk

Abstract: In this article, we describe a series of new complex salts in which electron-donating *cis*-$\{Ru^{II}(NH_3)_4\}^{2+}$ centers are connected to two electron-accepting *N*-methyl/aryl-pyridinium groups. These V-shaped complexes contain either monodentate 4,4′-bipyridyl-derived ligands or related chelates based on 2,2′:4,4″:4′,4‴-quaterpyridyl and have been characterized by using various techniques including electronic absorption spectroscopy and cyclic voltammetry. Molecular quadratic nonlinear optical (NLO) responses β have been determined by using hyper-Rayleigh scattering at 800 nm and also via Stark (electroabsorption) spectroscopic studies on the intense, visible d $\rightarrow \pi^*$ metal-to-ligand charge-transfer bands. These experiments reveal that these dipolar pseudo-C_{2v} chromophores exhibit two substantial components of the β tensor, β_{zzz} and β_{zyy}, with the difference between them being most marked for the nonchelated systems. Time-dependent density-functional theory and finite field calculations serve to further illuminate the electronic structures and associated linear and NLO properties of the new chromophoric salts.

Introduction

Nonlinear optical (NLO) materials based on molecular compounds are of considerable current interest because they hold promise for applications in advanced optoelectronic and all-optical data processing technologies.[1] Fundamental research in this area has recently featured an increasing number of studies on organotransition metal complexes which offer greater scope for the creation of multifunctional NLO materials when compared with purely organic compounds.[2] Quadratic (second-order) NLO properties, which are of the most immediate interest for practical applications, derive at the molecular level from first hyperpolarizabilities β. The majority of chromophores studied to date, whether metal-containing or purely organic, contain an electron donor group (D) connected to an electron acceptor (A) via a polarizable π-conjugated bridge. The molecular optical nonlinearities of such simple dipolar species are largely one-dimensional (1D) in nature, i.e. dominated by one β tensor component. Introducing multiple D and/or A groups increases the number of significant components of β, which then acquires a greater degree of multidimensional (MD) character.

† University of Manchester.
‡ Brookhaven National Laboratory.
§ University of Leuven.
|| Universidad de Zaragoza.
University of Southampton.
⊥ Present address: Molecular Materials Research Center, Beckman Institute, MC 139-74, California Institute of Technology, 1200 East California Blvd., Pasadena, CA 91125.

(1) (a) *Nonlinear Optical Properties of Organic Molecules and Crystals*; Chemla, D. S., Zyss, J., Eds.; Academic Press: Orlando, FL, 1987; Vols. 1 and 2. (b) Zyss, J. *Molecular Nonlinear Optics: Materials, Physics and Devices*; Academic Press: Boston, 1994. (c) *Organic Nonlinear Optical Materials*; Bosshard, Ch., Sutter, K., Prêtre, Ph., Hulliger, J., Flörsheimer, M., Kaatz, P., Günter, P., Eds.; Advances in Nonlinear Optics, Vol. 1; Gordon & Breach: Amsterdam, The Netherlands, 1995. (d) *Nonlinear Optics of Organic Molecules and Polymers*; Nalwa, H. S., Miyata, S., Eds.; CRC Press: Boca Raton, FL, 1997.

(2) (a) Nalwa, H. S. *Appl. Organomet. Chem.* **1991**, *5*, 349−377. (b) Marder, S. R. In *Inorganic Materials*, 2nd ed.; Bruce, D. W., O'Hare, D., Eds.; Wiley: Chichester; 1992; pp 121−169. (c) Kanis, D. R.; Ratner, M. A.; Marks, T. J. *Chem. Rev.* **1994**, *94*, 195−242. (d) Long, N. J. *Angew. Chem., Int. Ed. Engl*. **1995**, *34*, 21−38. (e) Whittall, I. R.; McDonagh, A. M.; Humphrey M. G.; Samoc, M. *Adv. Organomet. Chem*. **1998**, *42*, 291−362. (f) Whittall, I. R.; McDonagh, A. M.; Humphrey M. G.; Samoc, M. *Adv. Organomet. Chem*. **1998**, *43*, 349−405. (g) Heck, J.; Dabek, S.; Meyer-Friedrichsen, T.; Wong, H. *Coord. Chem. Rev*. **1999**, *190−192*, 1217−1254. (h) Gray, G. M.; Lawson, C. M. In *Optoelectronic Properties of Inorganic Compounds*; Roundhill, D. M.; Fackler, J. P., Jr., Eds.; Plenum: New York, 1999; pp. 1−27. (i) Shi, S. In *Optoelectronic Properties of Inorganic Compounds*; Roundhill, D. M.; Fackler, J. P., Jr., Eds.; Plenum: New York, 1999; pp. 55−105. (j) Le Bozec, H.; Renouard, T. *Eur. J. Inorg. Chem.* **2000**, 229−239. (k) Barlow, S.; Marder, S. R. *Chem. Commun*. **2000**, 1555−1562. (l) Lacroix, P. G. *Eur. J. Inorg. Chem*. **2001**, 339−348. (m) Di Bella, S. *Chem. Soc. Rev*. **2001**, *30*, 355−366. (n) Coe, B. J. In *Comprehensive Coordination Chemistry II*; McCleverty J. A., Meyer, T. J., Eds.; Elsevier Pergamon: Oxford, 2004; Vol. 9, pp 621−687.

Various organic MD NLO compounds have recently emerged as candidates for quadratic applications,[3] offering potential advantages over 1D chromophores such as increased β responses without undesirable losses of transparency in the visible region. Of particular relevance to the present report, it has been shown that off-diagonal tensor components of β can become significant in dipolar molecules with C_{2v} symmetry that display electronic transitions for which the direction of the transition dipole moment μ_{12} is perpendicular to the C_2 axis.[3a] Examples of such molecules include (dicyanomethylene)pyran derivatives[3d,i] or asymmetrically substituted 1,3,5-tris(phenylethynyl)benzenes;[3f,h] compounds of this type are attractive for electrooptic applications and also offer new possibilities for achieving phase-matched second harmonic generation. A relatively small number of neutral dipolar 2D metal complexes have also been studied,[2l,4] in particular Schiff base derivatives, but to our knowledge no related charged metallochromophores have yet been investigated for their NLO properties.

We have previously described systematic studies on 1D ruthenium ammine complex salts which possess very large NLO responses that are tunable by ligand-based changes[5] and also reversibly switchable via $Ru^{III/II}$ redox.[6] The latter general observation is particularly significant because it provides a key incentive for incorporating Ru^{II} ammine centers into NLO chromophores. We have now employed similar design strategies in the creation of two series of novel dipolar 2D C_{2v} chromophores, each of which features a *cis*-$\{Ru^{II}(NH_3)_4\}^{2+}$ D center connected to two pyridinium A groups. A number of salts of related trans complexes have also been prepared; although such centrosymmetric or pseudocentrosymmetric species are not expected to possess substantial β responses, they are of interest largely for comparison of their spectroscopic and electrochemical properties with those of the cis species. The molecular quadratic NLO properties of our new compounds have been assessed directly by using the hyper-Rayleigh scattering (HRS) technique[7] and also indirectly via electronic Stark effect (electroabsorption) spectroscopy.[8] In addition, time-dependent density functional theory (TD-DFT) and finite field calculations have been carried out to further illuminate the electronic structures of the complexes studied. Some of the experimental results described herein for the nonchelated *cis*-$\{Ru^{II}(NH_3)_4\}^{2+}$ complex salts have been previously communicated.[9]

Experimental Section

Materials and Procedures. All reactions were performed under an Ar atmosphere and in Ar-purged solvents. All reactions and chromatographic purifications involving complex salts were performed in the dark. The compounds *cis*-$[Ru^{III}Cl_2(NH_3)_4]Cl$,[10] *trans*-$[Ru^{II}Cl(NH_3)_4(SO_2)]Cl$,[11] $[Ru^{II}(NH_3)_5(H_2O)][PF_6]_2$,[11] $[MeQ^+]I$,[5a] $[PhQ^+]Cl\cdot 2H_2O$,[5c] $[4\text{-}AcPhQ^+]Cl\cdot 2H_2O$,[5c] $[2\text{-}PymQ^+]Cl$,[5d] and *N*″,*N*‴-dimethyl-2,2′:4,4″:4′,4‴-quaterpyridinium hexafluorophosphate ($[Me_2Qpy^{2+}][PF_6]_2$)[12] were synthesized by previously published methods. All other reagents were obtained commercially and used as supplied. Products were dried overnight in a vacuum desiccator ($CaSO_4$) prior to characterization.

General Physical Measurements. ^1H NMR spectra were recorded on a Varian Gemini 200 spectrometer, and all shifts are referenced to TMS. The fine splitting of pyridyl or phenyl ring AA′BB′ patterns is ignored, and the signals are reported as simple doublets, with *J* values referring to the two most intense peaks. Elemental analyses were performed by the Microanalytical Laboratory, University of Manchester and UV/VIS spectra were obtained by using a Hewlett-Packard 8452A diode array spectrophotometer. Infrared spectroscopy was performed on nondiluted samples using an Excalibur BioRad FT-IR spectrometer equipped with a Golden Gate attenuated total reflectance accessory.

Cyclic and differential pulse voltammetric measurements were performed on a BAS CV50W voltammetric analyzer. A single-compartment cell was used with a silver/silver chloride reference electrode separated by a salt bridge from a Pt disk working electrode and Pt wire auxiliary electrode. Acetonitrile was freshly distilled (from CaH_2), and $[NBu^n_4]PF_6$, twice recrystallized from ethanol, and dried in vacuo, was used as the supporting electrolyte. Solutions containing ca. 10^{-3} M analyte (0.1 M electrolyte) were deaerated by purging with N_2. All $E_{1/2}$ values were calculated from $(E_{pa} + E_{pc})/2$ at a scan rate of 200 mV s^{-1}.

Synthesis of 2,2′:4,4″:4′,4‴-Quaterpyridyl (Qpy). A mixture of 4,4′-bipyridyl (20 g, 128 mmol) and 10% Pd on charcoal (4 g) was heated at ca. 250 °C for 48 h and then cooled to room temperature.

(3) Selected examples: (a) Wortmann, R.; Krämer, P.; Glania, C.; Lebus S.; Detzer, N. *Chem. Phys.* **1993**, *173*, 99−108. (b) Zyss, J. *J. Chem. Phys.* **1993**, *98*, 6583−6599. (c) Zyss J.; Ledoux, I. *Chem. Rev.* **1994**, *94*, 77−105. (d) Moylan, C. R.; Ermer, S.; Lovejoy, S. M.; McComb, I.-H.; Leung, D. S.; Wortmann, R.; Krdmer P.; Twieg, R. J. *J. Am. Chem. Soc.* **1996**, *118*, 8, 12950−12955. (e) Wortmann, R.; Glania, C.; Krämer, P.; Matschiner, R.; Wolff, J. J.; Kraft, S.; Treptow, B.; Barbu, E.; Längle D.; Görlitz, G. *Chem. Eur. J.* **1997**, *3*, 1765−1773. (f) Wolff, J. J.; Längle, D.; Hillenbrand, D.; Wortmann, R.; Matschiner, R.; Glania, C.; Krämer, P. *Adv. Mater*. **1997**, *9*, 138−143. (g) Tomonari, M.; Ookubo N.; Takada, T. *Chem. Phys. Lett.* **1997**, *266*, 488−498. (h) Wolff J. J.; Wortmann, R. *Adv. Phys. Org. Chem*. **1999**, *32*, 121−217. (i) Liu, Y.-J.; Liu, Y.; Zhang, D.-J.; Hu, H.-Q.; Liu, C.-B. *J. Mol. Struct*. **2001**, *570*, 43−51. (j) Ostroverkhov, V.; Petschek, R. G.; Singer, K. D.; Twieg, R. J. *Chem. Phys. Lett*. **2001**, *340*, 109−115. (k) Yang M.-L.; Champagne, B. *J. Phys. Chem. A* **2003,** *107*, 3942−3951. (l) Wortmann, R.; Lebus-Henn, S.; Reis, H.; Papadopoulos, M. G. *J. Mol. Struct. (THEOCHEM)* **2003**, *633*, 217−226.

(4) Selected examples: (a) Lacroix, P. G.; Di Bella, S.; Ledoux, I. *Chem. Mater.* **1996**, *8*, 541−545. (b) Di Bella, S.; Fragalà, I.; Ledoux, I.; Diaz-Garcia, M. A.; Marks, T. J. *J. Am. Chem. Soc.* **1997**, *119*, 9550−9557. (c) Averseng, F.; Lacroix, P. G.; Malfant, I.; Lenoble, G.; Cassoux, P.; Nakatani, K.; Maltey-Fanton, I.; Delaire, J. A.; Aukauloo, A. *Chem. Mater*. **1999**, *11*, 995−1002. (d) Briel, O.; Sünkel, K.; Krossing, I.; Nöth, H.; Schmälzlin, E.; Meerholz, K.; Bräuchle, C.; Beck, W. *Eur. J. Inorg. Chem*. **1999**, 483−490. (e) Hilton, A.; Renouard, T.; Maury, O.; Le Bozec, H.; Ledoux, I.; Zyss, J. *Chem. Commun*. **1999**, 2521−2522. (f) Di Bella, S.; Fragalà, I.; Ledoux, I.; Zyss, J. *Chem. Eur. J.* **2001**, *7*, 3738−3743. (g) Di Bella, S.; Fragalà, I. *New J. Chem.* **2002**, *26*, 285−290. (h) Di Bella, S.; Fragalà, I. *Eur. J. Inorg. Chem*. **2003**, 2606−2611. (i) Maya, E. M.; García-Frutos, E. M.; Vázquez, P.; Torres, T.; Martín, G.; Rojo, G.; Agulló-López, F.; González-Jonte, R. H.; Ferro, V. R.; García de la Vega, J. M.; Ledoux, I.; Zyss, J. *J. Phys. Chem. A* **2003,** *107*, 2110−2117. (j) Di Bella, S.; Fragalà, I.; Guerri, A.; Dapporto, P.; Nakatani, K. *Inorg. Chim. Acta* **2004**, *357*, 1161−1167.

(5) (a) Coe, B. J.; Chamberlain, M. C.; Essex-Lopresti, J. P.; Gaines, S.; Jeffery, J. C.; Houbrechts, S.; Persoons, A. *Inorg. Chem*. **1997**, *36*, 3284−3292. (b) Coe, B. J.; Essex-Lopresti, J. P.; Harris, J. A.; Houbrechts S.; Persoons, A. *Chem. Commun.* **1997**, 1645−1646. (c) Coe, B. J.; Harris, J. A.; Harrington, L. J.; Jeffery, J. C.; Rees, L. H.; Houbrechts S.; Persoons, A. *Inorg. Chem*. **1998**, *37*, 3391−3399. (d) Coe, B. J.; Harris, J. A.; Asselberghs, I.; Persoons, A.; Jeffery, J. C.; Rees, L. H.; Gelbrich T.; Hursthouse, M. B. *J. Chem. Soc., Dalton Trans*. **1999**, 3617−3625. (e) Coe, B. J.; Harris, J. A.; Brunschwig, B. S. *J. Phys. Chem. A* **2002**, *106*, 897−905. (f) Coe, B. J.; Jones, L. A.; Harris, J. A.; Brunschwig, B. S.; Asselberghs, I.; Clays, K.; Persoons, A. *J. Am. Chem. Soc.* **2003**, *125*, 862−863. (g) Coe, B. J.; Jones, L. A.; Harris, J. A.; Sanderson, E. E.; Brunschwig, B. S.; Asselberghs, I.; Clays, K.; Persoons, A. *Dalton Trans*. **2003**, 2335−2341. (h) Coe, B. J.; Jones, L. A.; Harris, J. A.; Brunschwig, B. S.; Asselberghs, I.; Clays, K.; Persoons, A.; Garín, J.; Orduna, J. *J. Am. Chem. Soc.* **2004**, *126*, 3880−3891.

(6) (a) Coe, B. J.; Houbrechts, S.; Asselberghs I.; Persoons, A. *Angew. Chem., Int. Ed.* **1999**, *38*, 366−369. (b) Coe, B. J. *Chem. Eur. J.* **1999**, *5*, 2464−2471.

(7) (a) Terhune, R. W.; Maker, P. D.; Savage, C. M. *Phys. Rev. Lett*. **1965**, *14*, 681−684. (b) Clays, K.; Persoons, A. *Phys. Rev. Lett*. **1991**, *66*, 2980−2983. (c) Clays, K.; Persoons, A. *Rev. Sci. Instrum*. **1992**, *63*, 3285−3289. (d) Hendrickx, E.; Clays, K.; Persoons, A. *Acc. Chem. Res.* **1998**, *31*, 675−683.

(8) (a) Liptay, W. In *Excited States*; Lim, E. C., Ed.; Academic Press: New York, 1974; Vol. 1, pp 129−229. (b) Bublitz, G. U.; Boxer, S. G. *Annu. Rev. Phys. Chem.* **1997**, *48*, 213−242.

(9) Coe, B. J.; Harris, J. A.; Brunschwig, B. S. *Dalton Trans*. **2003**, 2384−2386.

(10) Boggs, S. E.; Clarke R. E.; Ford, P. C. *Inorg. Chim. Acta* **1996**, *247*, 129−130.

(11) Curtis, J. C.; Sullivan, B. P.; Meyer, T. J. *Inorg. Chem*. **1983**, *22*, 224−236.

(12) Morgan R. J.; Baker, A. D. *J. Org. Chem*. **1990**, *55*, 1986−1993.

HCl (2 M, 500 mL) was added, and the resulting black suspension was filtered. Dropwise addition of aqueous NaOH (8 M) to the stirred filtrate gave a cream precipitate which was filtered off, washed with water, and dried. This solid was then loaded into a Soxhlet and extracted with acetone (4 × 400 mL portions) over several days. Each portion was treated as follows: any precipitate was filtered off and dried, and the filtrate was also evaporated to dryness. Both of the resulting solids were then analyzed by ^{1}H NMR, and materials with similar spectra were combined. Compounds were extracted in the order of their acetone solubility, i.e. unreacted 4,4′-bpy first, followed by Qpy, and then higher-order oligomers. The combined Qpy crops were heated at reflux in $CHCl_3$ (300 mL) in the presence of activated charcoal (3 g) and concentrated HCl (5 drops) for 1 h. The resulting mixture was cooled to room temperature, filtered though Celite 545, and evaporated to dryness to give a white powder: 7.48 g, 37%; δ_H ($CDCl_3$) 8.82 (2 H, d, J = 5.1 Hz, C_5H_3N), 8.79−8.76 (6 H, m, C_5H_3N + C_5H_4N), 7.68 (4 H, d, J = 6.1 Hz, C_5H_4N), 7.60 (2 H, dd, J = 1.8, 5.1 Hz, C_5H_3N). Anal. Calcd (%) for $C_{20}H_{14}N_4 \cdot 0.5H_2O$: C, 75.22; H, 4.73; N, 17.54. Found: C, 75.03; H, 4.42; N, 17.38.

Synthesis of *N*″,*N*‴-Diphenyl-2,2′:4,4″:4′,4‴-quaterpyridinium Hexafluorophosphate [Ph_2Qpy^{2+}][PF_6]$_2$. A mixture of Qpy·0.5H_2O (100 mg, 0.31 mmol) and 2,4-dinitrochlorobenzene (607 mg, 3.00 mmol) in ethanol (25 mL) was heated at reflux for 48 h. Addition of diethyl ether produced a gray precipitate which was filtered off, washed with diethyl ether, and dried to yield crude *N*″,*N*‴-di(2,4-dinitrophenyl)-2,2′:4,4″:4′4‴-quaterpyridinium chloride ([(2,4-DNPh)$_2$$Qpy^{2+}$]$Cl_2$). This material was dissolved in DMSO (5 mL), and aniline (0.3 mL, 3.30 mmol) was added. The resulting solution was heated at 70 °C for 3 h, cooled, and then filtered. Acetone was added to the filtrate, and a white precipitate was filtered off, washed with acetone, and dried. The solid was dissolved in water, and aqueous NH_4PF_6 was added to give a white precipitate. The product as filtered off, washed with water, and dried: 154 mg, 66%; δ_H (CD_3COCD_3) 9.61 (4 H, d, J = 7.0 Hz, C_5H_4N), 9.15 (2 H, d, J = 1.2 Hz, C_5H_3N), 9.11 (2 H, d, J = 5.1 Hz, C_5H_3N), 9.00 (4 H, d, J = 7.0 Hz, C_5H_4N), 8.25 (2 H, dd, J = 1.9, 5.1 Hz, C_5H_3N), 8.09−8.04 (4 H, m, Ph), 7.87−7.84 (6 H, m, Ph). Anal. Calcd (%) for $C_{32}H_{24}F_{12}N_4P_2$: C, 50.94; H, 3.21; N, 7.43. Found: C, 50.40; H, 2.91; N, 7.24.

Synthesis of *N*″,*N*‴-Di(4-acetylphenyl)-2,2′:4,4″:4′,4‴-quaterpyridinium Hexafluorophosphate [(4-AcPh)$_2$$Qpy^{2+}$][$PF_6$]$_2$. This was prepared in a manner similar to [Ph_2Qpy^{2+}][PF_6]$_2$ by using 4-acetophenone (406 mg, 3.00 mmol) instead of aniline, with heating at reflux in ethanol (50 mL) for 50 h. The resulting solution was reduced to a small volume, acetone was added, and a brown precipitate was filtered off. The solid was dissolved in water, and aqueous NH_4PF_6 was added to give a light-brown precipitate. The product was filtered off, washed with water, and dried. Further purification was achieved by reprecipitation from acetone/diethyl ether: 71 mg, 26%; δ_H (CD_3COCD_3) 9.67 (4 H, d, J = 7.0 Hz, C_5H_4N), 9.16 (2 H, d, J = 1.2 Hz, C_5H_3N), 9.12 (2 H, d, J = 5.1 Hz, C_5H_3N), 9.04 (4 H, d, J = 7.0 Hz, C_5H_4N), 8.41 (4 H, d, J = 8.8 Hz, C_6H_4), 8.27−8.20 (6 H, m, C_5H_3N + C_6H_4), 2.74 (6 H, s, Me). ν(C═O) 1686 cm^{-1}. Anal. Calcd (%) for $C_{36}H_{28}F_{12}N_4O_2P_2 \cdot 1.5H_2O$: C, 49.95; H, 3.61; N, 6.47. Found: C, 49.45; H, 3.27; N, 6.76.

Synthesis of *N*″,*N*‴-Di(2-pyrimidyl)-2,2′:4,4″:4′,4‴-quaterpyridinium Hexafluorophosphate [(2-Pym)$_2$$Qpy^{2+}$][$PF_6$]$_2$. A mixture of Qpy·0.5$H_2O$ (100 mg, 0.31 mmol) and 2-chloropyrimidine (359 mg, 3.13 mmol) was heated quickly to 120 °C to produce a white solution which turned green after 10 min. Ethanol (3 mL) was added and the suspension heated at reflux for 4 h. Diethyl ether (50 mL) was added, and a white precipitate was filtered off, washed with diethyl ether, and dried. The solid was dissolved in water, and aqueous NH_4PF_6 was added to give a white precipitate. The product as filtered off, washed with water, and dried: 226 mg, 96%; δ_H (CD_3COCD_3) 10.44 (4 H, d, J = 7.2 Hz, C_5H_4N), 9.33 (4 H, d, J = 4.8 Hz, $C_4H_3N_2$), 9.21 (2 H, s, C_5H_3N), 9.15 (2 H, d, J = 5.1 Hz, C_5H_3N), 9.09 (4 H, d, J = 7.3 Hz, C_5H_4N), 8.31 (2 H, dd, J = 1.9, 5.1 Hz, C_5H_3N), 8.08 (2 H, t, J = 4.9 Hz, $C_4H_3N_2$). Anal. Calcd (%) for $C_{28}H_{20}F_{12}N_8P_2$: C, 44.34; H, 2.66; N, 14.77. Found: C, 44.67; H, 2.59; N, 14.50.

Synthesis of *cis*-[$Ru^{II}(NH_3)_4(MeQ^+)_2$][PF_6]$_4$ (1). A solution of *cis*-[$Ru^{III}Cl_2(NH_3)_4$]Cl (55 mg, 0.200 mmol) in degassed water (5 mL) acidified with trifluoroacetic acid (3 drops) was reduced over zinc amalgam (5 lumps) for 15 min with argon agitation. The solution was filtered under argon into a flask containing [MeQ^+]I (298 mg, 1.00 mmol), and the reaction was stirred in the dark under argon for 5 h. Acetone (850 mL) was added, and the crude halide salt product was collected by filtration, washed with acetone, and dried. This material was metathesized using water/aqueous NH_4PF_6 to yield a dark-purple solid. Purification was achieved by precipitation from acetone/aqueous NH_4PF_6: 109 mg, 49%; δ_H (CD_3COCD_3) 9.12 (4 H, d, J = 6.9 Hz, 2C_5H_4N), 8.88 (4 H, d, J = 6.9 Hz, 2C_5H_4N), 8.66 (4 H, d, J = 7.0 Hz, 2C_5H_4N), 7.95 (4 H, d, J = 6.9 Hz, 2C_5H_4N), 4.61 (6 H, s, 2Me), 3.39 (6 H, s, 2NH_3), 2.99 (s, 6 H, 2NH_3). Anal. Calcd (%) for $C_{22}H_{34}F_{24}N_8P_4Ru \cdot 1.5H_2O$: C, 23.62; H, 3.33; N, 10.02. Found: C, 23.69; H, 3.19; N, 9.63.

Synthesis of *cis*-[$Ru^{II}(NH_3)_4(PhQ^+)_2$][PF_6]$_4$ (2). This was prepared in manner similar to **1** by using [PhQ^+]Cl·2H_2O (305 mg, 1.00 mmol) in place of [MeQ^+]I. Acetone (150 mL) was added to precipitate the crude chloride product. Purification was achieved by sequential precipitations from acetone/diethyl ether to afford a dark-blue solid: 120 mg, 49%; δ_H (CD_3COCD_3) 9.42 (4 H, d, J = 7.2 Hz, 2C_5H_4N), 8.95 (4 H, d, J = 6.9 Hz, 2C_5H_4N), 8.84 (4 H, d, J = 7.2 Hz, 2C_5H_4N), 8.05 (4 H, d, J = 7.0 Hz, 2C_5H_4N), 8.01−7.96 (4 H, m, 2Ph), 7.85−7.79 (6 H, m, 2Ph), 3.45 (6 H, s, 2NH_3), 3.04 (6 H, s, 2NH_3). Anal. Calcd (%) for $C_{32}H_{38}F_{24}N_8P_4Ru \cdot 0.5H_2O$: C, 31.38; H, 3.21; N, 9.15. Found: C, 31.34; H, 3.24; N, 9.01.

Synthesis of *cis*-[$Ru^{II}(NH_3)_4$(4-$AcPhQ^+$)$_2$][PF_6]$_4$ (3). This was prepared and purified in manner similar to **1** by using [4-$AcPhQ^+$]Cl·2H_2O (347 mg, 1 mmol) in place of [MeQ^+]I. Acetone (100 mL) was added to precipitate the crude chloride product. A dark-blue solid was obtained: 121 mg, 46%; δ_H (CD_3COCD_3) 9.47 (4 H, d, J = 6.9 Hz, 2C_5H_4N), 8.95 (4 H, d, J = 6.8 Hz, 2C_5H_4N), 8.87 (4 H, d, J = 6.8 Hz, 2C_5H_4N), 8.36 (4 H, d, J = 8.8 Hz, 2C_6H_4), 8.15 (4 H, d, J = 8.8 Hz, 2C_6H_4), 8.05 (4 H, d, J = 6.8 Hz, 2C_5H_4N), 3.46 (6 H, s, 2NH_3), 3.05 (6 H, s, 2NH_3), 2.72 (6 H, s, 2Me). ν(C═O) 1686 cm^{-1}. Anal. Calcd (%) for $C_{36}H_{42}F_{24}N_8O_2P_4Ru \cdot H_2O$: C, 32.81; H, 3.37; N, 8.50. Found: C, 32.92; H, 2.87; N, 8.26.

Synthesis of *cis*-[$Ru^{II}(NH_3)_4$(2-$PymQ^+$)$_2$][PF_6]$_4$ (4). This was prepared and purified in manner similar to **3** by using [2-$PymQ^+$]Cl (271 mg, 1 mmol) in place of [4-$AcPhQ^+$]Cl·2H_2O. Further purification was achieved by precipitation from acetone/aqueous NH_4PF_6 to afford a dark-blue solid: 64 mg, 26%; δ_H (CD_3COCD_3) 10.26 (4 H, d, J = 7.3 Hz, 2C_5H_4N), 9.27 (4 H, d, J = 4.8 Hz, 2$C_4H_3N_2$), 9.01−8.92 (8 H, m, 4C_5H_4N), 8.11 (4 H, d, J = 7.0 Hz, 2C_5H_4N), 8.04 (2 H, t, J = 4.9 Hz, 2$C_4H_3N_2$), 3.53 (6 H, s, 2NH_3), 3.09 (6 H, s, 2NH_3). Anal. Calcd (%) for $C_{28}H_{34}F_{24}N_{12}P_4Ru \cdot H_2O$: C, 27.17; H, 2.93; N, 13.58. Found: C, 27.13; H, 2.64; N, 13.13.

Synthesis of *trans*-[$Ru^{II}(NH_3)_4(MeQ^+)_2$][PF_6]$_4$ (5). A mixture of *trans*-[$Ru^{II}Cl(NH_3)_4(SO_2)$]Cl (100 mg, 0.329 mmol) and [MeQ^+]I (196 mg, 0.657 mmol) was dissolved in water (5 mL) and heated at ca. 50 °C under argon for 30 min. Acetone (30 mL) was added to the brown solution, and a brown precipitate was filtered off, washed with acetone, and dried. This material (a mixture of chloride or iodide salts of *trans*-[$Ru^{II}(NH_3)_4(SO_2)(MeQ^+)]^{3+}$ and unreacted [MeQ^+]I) was dissolved in water (5 mL) and oxidized by the addition of a 1:1 mixture of 30% aqueous H_2O_2/2M HCl (3 mL). After 5 min at room temperature, a brown precipitate was filtered off, washed with water, and discarded. Acetone (200 mL) was added to the filtrate, and a golden-yellow precipitate was filtered off, washed with acetone, and dried to afford *trans*-[$Ru^{III}(SO_4)(NH_3)_4(MeQ^+)$]$Cl_2$. This product was dissolved in water (5 mL) and reduced over zinc amalgam (5 lumps) with argon agitation for 15 min. The deep-blue solution was then filtered under

argon into a flask containing [MeQ$^+$]I (196 mg, 0.657 mmol), and the solution was stirred at room temperature in the dark under argon for 24 h. The addition of acetone (100 mL) to the deep-blue solution gave a dark precipitate which was filtered off, washed with acetone, and dried. This crude material was reprecipitated from water/aqueous NH_4PF_6. Further purification was effected by precipitation from acetone/aqueous NH_4PF_6 and then from acetone/diethyl ether to afford a dark-purple solid: 188 mg, 52%; δ_H (CD_3COCD_3) 9.21 (4 H, d, J = 6.9 Hz, 2C_5H_4N), 9.19 (4 H, d, J = 7.2 Hz, 2C_5H_4N), 8.73 (4 H, d, J = 7.0 Hz, 2C_5H_4N), 8.16 (4 H, d, J = 6.9 Hz, 2C_5H_4N), 4.65 (6 H, s, 2Me), 2.90 (12 H, s, 4NH_3). Anal. Calcd (%) for $C_{22}H_{34}F_{24}N_8P_4Ru$: C, 24.21; H, 3.14; N, 10.27. Found: C, 24.34; H, 3.27; N, 10.11.

Synthesis of *trans*-[Ru^{II}(NH$_3$)$_4$(PhQ$^+$)$_2$][PF$_6$]$_4$ (6). This was prepared and purified in manner similar to **5**, by using [PhQ$^+$]Cl·2H_2O (200 mg, 0.656 mmol) instead of [MeQ$^+$]I. Following the oxidation step, no brown precipitate was produced and the *trans*-[Ru^{III}(SO$_4$)(NH$_3$)$_4$(PhQ$^+$)]Cl$_2$ intermediate was precipitated with acetone (100 mL). A dark-blue solid was obtained: 159 mg, 39%; δ_H (CD_3COCD_3) 9.49 (4 H, d, J = 7.1 Hz, 2C_5H_4N), 9.27 (4 H, d, J = 6.8 Hz, 2C_5H_4N), 8.92 (4 H, d, J = 7.1 Hz, 2C_5H_4N), 8.26 (4 H, d, J = 6.8 Hz, 2C_5H_4N), 8.04−7.98 (4 H, m, 2Ph), 7.84−7.81 (6 H, m, 2Ph), 2.94 (12 H, s, 4NH_3). Anal. Calcd (%) for $C_{32}H_{38}F_{24}N_8P_4Ru·H_2O$: C, 31.16; H, 3.27; N, 9.08. Found: C, 31.05; H, 3.25; N, 8.76.

Synthesis of *trans*-[Ru^{II}(NH$_3$)$_4$(4-AcPhQ$^+$)$_2$][PF$_6$]$_4$ (7). This was prepared and purified in manner similar to **6**, by using [4-AcPhQ$^+$]Cl·2H_2O (228 mg, 0.657 mmol) instead of [PhQ$^+$]Cl·2H_2O. A dark-blue solid was obtained: 123 mg, 29%; δ_H (CD_3COCD_3) 9.54 (4 H, d, J = 7.0 Hz, 2C_5H_4N), 9.27 (4 H, d, J = 6.7 Hz, 2C_5H_4N), 8.94 (4 H, d, J = 7.0 Hz, 2C_5H_4N), 8.38 (4 H, d, J = 8.8 Hz, 2C_6H_4), 8.27 (4 H, d, J = 6.7 Hz, 2C_5H_4N), 8.17 (4 H, d, J = 8.7 Hz, 2C_6H_4), 2.95 (12 H, s, 4NH_3), 2.86 (6 H, s, 2Me). Anal. Calcd (%) for $C_{36}H_{42}F_{24}N_8O_2P_4Ru$: C, 33.27; H, 3.26; N, 8.62. Found: C, 33.27; H, 3.36; N, 8.25.

Synthesis of *trans*-[Ru^{II}(NH$_3$)$_4$(2-PymQ$^+$)$_2$][PF$_6$]$_4$ (8). This was prepared and purified in manner similar to **6**, by using [2-PymQ$^+$]Cl (178 mg, 0.658 mmol) instead of [PhQ$^+$]Cl·2H_2O. A dark-blue solid was obtained: 176 mg, 43%; δ_H (CD_3COCD_3) 10.32 (4 H, d, J = 7.3 Hz, 2C_5H_4N), 9.32 (4 H, d, J = 6.9 Hz, 2C_5H_4N), 9.29 (4 H, d, J = 4.9 Hz, 2$C_4H_3N_2$), 9.00 (4 H, d, J = 7.3 Hz, 2C_5H_4N), 8.30 (4 H, d, J = 6.9 Hz, 2C_5H_4N), 8.04 (2 H, t, J = 4.9 Hz, 2$C_4H_3N_2$), 2.97 (12 H, s, 4NH_3). Anal. Calcd (%) for $C_{28}H_{34}F_{24}N_{12}P_4Ru·2H_2O$: C, 26.78; H, 3.05; N, 13.39. Found: C, 26.82; H, 2.79; N, 13.27.

Synthesis of *trans*-[Ru^{II}(NH$_3$)$_4$(MeQ$^+$)(PhQ$^+$)][PF$_6$]$_4$ (9). This was prepared and purified in manner similar to **5**, with the second portion of [MeQ$^+$]I replaced by [PhQ$^+$]Cl·2H_2O (200 mg, 0.656 mmol). A dark-purple solid was obtained: 130 mg, 34%; δ_H (CD_3COCD_3) 9.49 (2 H, d, J = 7.1 Hz, C_5H_4N), 9.27−9.18 (6 H, m, 3C_5H_4N), 8.91 (2 H, d, J = 7.2 Hz, C_5H_4N), 8.74 (2 H, d, J = 7.0 Hz, C_5H_4N), 8.24 (2 H, d, J = 6.9 Hz, C_5H_4N), 8.18 (2 H, d, J = 6.8 Hz, C_5H_4N), 8.04−7.99 (2 H, m, Ph), 7.84−7.81 (3 H, m, Ph), 4.66 (3 H, s, Me), 2.92 (12 H, s, 4NH_3). Anal. Calcd (%) for $C_{27}H_{36}F_{24}N_8P_4Ru$: C, 28.11; H, 3.15; N, 9.71. Found: C, 28.09; H, 3.10; N, 9.50.

Synthesis of *trans*-[Ru^{II}(NH$_3$)$_4$(MeQ$^+$)(4-AcPhQ$^+$)][PF$_6$]$_4$ (10). This was prepared and purified in manner similar to **5**, with the second portion of [MeQ$^+$]I replaced by [4-AcPhQ$^+$]Cl·2H_2O (228 mg, 0.657 mmol). A dark-purple solid was obtained: 124 mg, 32%; δ_H (CD_3COCD_3) 9.53 (2 H, d, J = 7.2 Hz, C_5H_4N), 9.27−9.17 (6 H, m, 3C_5H_4N), 8.93 (2 H, d, J = 7.1 Hz, C_5H_4N), 8.74 (2 H, d, J = 7.0 Hz, C_5H_4N), 8.38 (2 H, d, J = 8.1 Hz, C_6H_4), 8.24 (2 H, d, J = 7.0 Hz, C_5H_4N), 8.18−8.14 (4 H, m, C_5H_4N + C_6H_4), 4.65 (3 H, s, Me), 2.92 (12 H, s, 4NH_3), 2.73 (3 H, s, C(O)Me). Anal. Calcd (%) for $C_{29}H_{38}F_{24}N_8OP_4Ru$: C, 29.13; H, 3.20; N, 9.37. Found: C, 28.84; H, 3.32; N, 9.23.

Synthesis of *trans*-[Ru^{II}(NH$_3$)$_4$(MeQ$^+$)(2-PymQ$^+$)][PF$_6$]$_4$ (11). This was prepared and purified in manner similar to **5**, with the second portion of [MeQ$^+$]I replaced by [2-PymQ$^+$]Cl (178 mg, 0.658 mmol). A dark-purple solid was obtained: 104 mg, 27%; δ_H (CD_3COCD_3) 10.31 (2 H, d, J = 7.1 Hz, C_5H_4N), 9.31−9.18 (8 H, m, 3C_5H_4N + $C_4H_3N_2$), 9.00 (2 H, d, J = 7.3 Hz, C_5H_4N), 8.74 (2 H, d, J = 6.9 Hz, C_5H_4N), 8.27 (2 H, d, J = 7.0 Hz, C_5H_4N), 8.19 (2 H, d, J = 6.8 Hz, C_5H_4N), 8.05 (1 H, t, J = 4.7 Hz, $C_4H_3N_2$), 4.66 (3 H, s, Me), 2.94 (12 H, s, 4NH_3). Anal. Calcd (%) for $C_{25}H_{34}F_{24}N_{10}P_4Ru$: C, 25.99; H, 2.97; N, 12.12. Found: C, 26.25; H, 2.79; N, 11.82.

Synthesis of [Ru^{II}(NH$_3$)$_4$(Me$_2$Qpy^{2+})][PF$_6$]$_4$ (12). A mixture of [Ru^{II}(NH$_3$)$_5$(H_2O)][PF$_6$]$_2$ (200 mg, 0.405 mmol) and [Me$_2$Qpy^{2+}][PF$_6$]$_2$ (255 mg, 0.405 mmol) in acetone (30 mL) was heated at reflux for 6 h in the dark under argon, cooled to room temperature, and filtered to remove unreacted ligand. The resulting filtrate was treated as outlined in purification method 1 below (three oxidation/reduction cycles), with further purification via precipitation from acetone/diethyl ether. A dark-purple solid was obtained: 71 mg, 16%; δ_H (CD_3COCD_3) 9.67 (2 H, d, J = 6.2 Hz, C_5H_3N), 9.17−9.14 (6 H, m, C_5H_3N + C_5H_4N), 8.82 (4 H, d, J = 6.9 Hz, C_5H_4N), 8.22 (2 H, dd, J = 2.2, 6.3 Hz, C_5H_3N), 4.67 (6 H, s, 2Me), 3.86 (6 H, s, 2NH_3), 2.49 (6 H, s, 2NH_3). Anal. Calcd (%) for $C_{22}H_{32}F_{24}N_8P_4Ru$: C, 24.25; H, 2.96; N, 10.29. Found: C, 23.82; H, 2.73; N, 10.04.

Synthesis of [Ru^{II}(NH$_3$)$_4$(Ph$_2$Qpy^{2+})][PF$_6$]$_4$ (13). This was prepared and purified in manner similar to **12** by using [Ph$_2$Qpy^{2+}][PF$_6$]$_2$ (305 mg, 0.404 mmol) instead of [Me$_2$Qpy^{2+}][PF$_6$]$_2$ and with only two oxidation/reduction cycles. A dark-purple solid was obtained: 123 mg, 25%; δ_H (CD_3COCD_3) 9.72 (2 H, d, J = 6.3 Hz, C_5H_3N), 9.44 (4 H, d, J = 7.1 Hz, C_5H_4N), 9.29 (2 H, d, J = 1.8 Hz, C_5H_3N), 8.98 (4 H, d, J = 6.7 Hz, C_5H_4N), 8.33 (2 H, dd, J = 1.9, 6.3 Hz, C_5H_3N), 8.03−7.98 (4 H, m, Ph), 7.85−7.81 (6 H, m, Ph) 3.91 (6 H, s, 2NH_3), 2.54 (6 H, s, 2NH_3). Anal. Calcd (%) for $C_{32}H_{36}F_{24}N_8P_4Ru$: C, 31.67; H, 2.99; N, 9.23. Found: C, 31.79; H, 2.97; N, 8.75.

Synthesis of [Ru^{II}(NH$_3$)$_4${(4-AcPh)$_2$Qpy^{2+}}][PF$_6$]$_4$ (14). This was prepared in manner similar to **12** by using [(4-AcPh)$_2$Qpy^{2+}][PF$_6$]$_2$·1.5H_2O (351 mg, 0.406 mmol) instead of [Me$_2$Qpy^{2+}][PF$_6$]$_2$. The initial filtrate was treated as outlined in purification method 2 below, to afford a dark-purple solid: 224 mg, 41%; δ_H (CD_3COCD_3) 9.73 (2 H, d, J = 6.4 Hz, C_5H_3N), 9.50 (4 H, d, J = 7.0 Hz, C_5H_4N), 9.30 (2 H, d, J = 1.6 Hz, C_5H_3N), 9.01 (4 H, d, J = 7.1 Hz, C_5H_4N), 8.41−8.32 (6 H, m, C_5H_3N + C_6H_4), 8.16 (4 H, d, J = 8.8 Hz, C_6H_4), 3.93 (6 H, s, 2NH_3), 2.74 (6 H, s, 2Me), 2.56 (6 H, s, 2NH_3). ν(C=O) 1686 cm^{-1}. Anal. Calcd (%) for $C_{36}H_{40}F_{24}N_8O_2P_4Ru·2H_2O$ C, 32.42; H, 3.33; N, 8.40. Found: C, 32.10; H, 3.29; N, 8.43.

Synthesis of [Ru^{II}(NH$_3$)$_4${(2-Pym)$_2$Qpy^{2+}}][PF$_6$]$_4$ (15). This was prepared in manner similar to **12** by using [(2-Pym)$_2$Qpy^{2+}][PF$_6$]$_2$ (307 mg, 0.405 mmol) instead of [Me$_2$Qpy^{2+}][PF$_6$]$_2$. The initial filtrate was treated as outlined in purification method 2 below, to afford a dark-purple solid: 89 mg, 18%; δ_H (CD_3COCD_3) 10.27 (4 H, d, J = 7.3 Hz, C_5H_4N), 9.76 (2 H, d, J = 6.3 Hz, C_5H_3N), 8.31−9.28 (6 H, m, C_5H_3N + $C_4H_3N_2$), 9.13 (4 H, d, J = 7.2 Hz, C_5H_4N), 8.38 (2 H, dd, J = 1.8, 6.5 Hz, C_5H_3N), 8.05 (2 H, t, J = 4.9 Hz, $C_4H_3N_2$), 3.97 (6 H, s, 2NH_3), 2.63 (6 H, s, 2NH_3). Anal. Calcd (%) for $C_{28}H_{32}F_{24}N_{12}P_4Ru·0.5Et_2O$: C, 28.72; H, 2.97; N, 13.40. Found: C, 28.56; H, 2.82; N, 13.14.

Purification Method 1. A solution of [NBu$^n_4$]I (0.15 M) was added dropwise to an acetone solution of the crude PF_6^- salt of the complex, and a dark purple precipitate was filtered off, washed with acetone, and dried. The resulting I^- salt was dissolved in a minimum of water, and a solution of 1:1 2 M HCl/30% aqueous H_2O_2 (25 mL) was added. After 1 h at room temperature, a brown precipitate was filtered off, and acetone (1.5 L) was added to the filtrate. After standing for 24 h, the dark precipitate was filtered off, washed with acetone, and dried. This crude Ru^{III} salt was dissolved in water (10 mL) and reduced over zinc amalgam (5 lumps) for 30 min with stirring. The zinc amalgam was removed by filtration and aqueous NH_4PF_6 was added dropwise to the filtrate to give a dark precipitate which was filtered off, washed with water, and dried. The ^{1}H NMR spectrum of the product at this stage was used as an indication of purity, and if necessary the oxidation/reduction cycle was repeated.

Purification Method 2. An acetone solution of the crude PF_6^- salt of the complex was loaded onto a silica gel column (230−400 mesh, 5 cm × 58 cm, 1 L dry gel) and eluted with NH_4PF_6 in acetonitrile (0.1 M). Fractions were collected and compared using thin-layer chromatography. Similar fractions were combined, reduced to dryness, and precipitated from acetone/aqueous NH_4PF_6. Further purification was achieved by precipitation from acetone/diethyl ether.

X-ray Crystallography. Crystals of the pro-ligand salt $[Ph_2Qpy^{2+}][PF_6]_2 \cdot Me_2CO$ were obtained by slow evaporation of an acetone solution. The pale-yellow plate crystal chosen for diffraction study had approximate dimensions of 0.50 mm × 0.30 mm × 0.06 mm. Data were collected on a Nonius Kappa CCD area-detector diffractometer controlled by the Collect software package.[13] The data were processed by Denzo[14] and corrected for absorption by using the empirical method employed in Sortav[15] from within the MaXus suite of programs.[16] The structure was solved by direct methods and refined by full-matrix least-squares on all F_0^2 data using SHELXS-97[17] and SHELXL-97.[18] All non-hydrogen atoms were refined anisotropically with hydrogen atoms included in idealized positions with thermal parameters riding on those of the parent atom. Crystallographic data and refinement details are presented in Table 3.

Hyper-Rayleigh Scattering. General details of the hyper-Rayleigh scattering (HRS) experiment have been discussed elsewhere,[7] and the experimental procedure and data analysis protocol used were as previously described.[19,20] Measurements were carried out in acetone or acetonitrile, with crystal violet as an external reference ($\beta_{xxx,800} = 500 \times 10^{-30}$ esu in acetonitrile; from the value of 340×10^{-30} esu in methanol,[20] corrected for local field factors at optical frequencies). All measurements were performed by using the 800 nm fundamental of a regenerative mode-locked Ti^{3+}:sapphire laser (Spectra Physics, model Tsunami, 100 fs pulses, 1 W, 80 MHz). Dilute solutions (10^{-5}−10^{-6} M) were used to ensure a linear dependence of $I_{2\omega}/I_\omega^2$ on solute concentration, precluding the need for Lambert−Beer correction factors. Samples were filtered (Millipore, 0.45 μm), and none showed any fluorescence. A relative error of ±15% is estimated for the β values determined via these measurements. HRS depolarization ratios[21] were determined at 800 nm in acetonitrile according to a published methodology.[22,23]

Stark Spectroscopy. The Stark apparatus, experimental methods and data collection procedure were as previously reported,[5e,24] except that a Xe arc lamp was used as the light source in the place of a W filament bulb. The Stark spectrum for each compound was measured a minimum of three times using different field strengths, and the signal was always found to be quadratic in the applied field. To fit the Stark data, the absorption (ϵ/ν vs ν) spectrum was modeled with a sum of Gaussian curves that reproduce the data and separate the peaks. The first and second derivatives of the Gaussian curves were then used to fit the Stark spectra with Liptay's equation.[8] The dipole moment change $\Delta\mu_{12}$ associated with each of the optical transitions considered in the fit was then calculated from the coefficient of the second derivative component. For all of the complexes two or three Gaussian functions were necessary to fit the absorption spectrum. In each case, only one or two of the Gaussian curves contributed the majority of the Stark signal, so the data yielded by the insignificant components have been neglected.

The Liptay equation is:[8]

$$\Delta\epsilon(\nu)/\nu = \left[A_\chi \epsilon(\nu)/\nu + \frac{B_\chi}{15h}\frac{\partial(\epsilon(\nu)/\nu)}{\partial\nu} + \frac{C_\chi}{30h^2}\frac{\partial^2(\epsilon(\nu)/\nu)}{\partial\nu^2}\right]\mathbf{F}_{\text{int}}^2 \quad (1)$$

where ν is the frequency of the light in Hz and the internal electric field is related to the applied external field by $\mathbf{F}_{\text{int}} = f_{\text{int}}\mathbf{F}_{\text{ext}}$. $\Delta\mu_{12}$ is related to the coefficient of the second derivative component by

$$C_\chi = 3\Delta\mu_{12}(2 - \cos^2\chi) + 3(m\Delta\mu_{12})^2(3\cos^2\chi - 1) \quad (2)$$

where $m\Delta\mu_{12}$ is the dipole moment change along the direction of the transition dipole moment μ_{12}. Butyronitrile was used as the glassing medium, for which the local field correction f_{int} is estimated as 1.33.[5e,24] A two-state analysis of the MLCT transitions gives

$$\Delta\mu_{\text{ab}}^2 = \Delta\mu_{12}^2 + 4\mu_{12}^2 \quad (3)$$

where $\Delta\mu_{\text{ab}}$ is the dipole moment change between the diabatic states and $\Delta\mu_{12}$ is the observed (adiabatic) dipole moment change. The value of μ_{12} can be determined from the oscillator strength f_{os} of the transition by

$$|\mu_{12}| = [f_{\text{os}}/(1.08 \times 10^{-5} E_{\max})]^{1/2} \quad (4)$$

where $E_{\max}$ is the energy of the MLCT maximum (in wavenumbers). The degree of delocalization c_b^2 and electronic coupling matrix element H_{ab} for the diabatic states are given by

$$c_b^2 = \frac{1}{2}\left[1 - \left(\frac{\Delta\mu_{12}^2}{\Delta\mu_{12}^2 + 4\mu_{12}^2}\right)^{1/2}\right] \quad (5)$$

$$|H_{\text{ab}}| = \left|\frac{E_{\max}(\mu_{12})}{\Delta\mu_{\text{ab}}}\right| \quad (6)$$

If the hyperpolarizability tensor β_0 has only nonzero elements along the CT direction, then this quantity is given by

$$\beta_0 = \frac{3\Delta\mu_{12}(\mu_{12})^2}{(E_{\max})^2} \quad (7)$$

A relative error of ±20% is estimated for the β_0 values derived from the Stark data and using eq 7.

Computational Procedures. All theoretical calculations were performed by using the Gaussian 03[25] program. The molecular geometries were optimized assuming C_{2v} symmetry (and also with no restrictions for the cation in **1**) by using the hybrid functional B3P86[26] and the LanL2DZ[27] basis set. It should be noted that quantum chemistry

(13) Hooft, R. *Collect*, Data collection software; Nonius BV: Delft, The Netherlands, 1998.
(14) Otwinowski, Z.; Minor, W. *Methods Enzymol*. **1997**, *276*, 307−326.
(15) (a) Blessing, R. H. *Acta Crystallogr., Sect. A* **1995**, *51*, 33−37. (b) Blessing, R. H. *J. Appl. Crystallogr*. **1997**, *30*, 421−426.
(16) Mackay, S.; Gilmore, C. J.; Edwards, C.; Tremayne, M.; Stewart, N.; Shankland, K. MAXUS, a computer program for the solution and refinement of crystal structures from diffraction data; University of Glasgow: Glasgow, U.K., Nonius BV, Delft, The Netherlands and MacScience Co. Ltd., Yokohama, Japan, 1998.
(17) Sheldrick, G. M. *Acta Crystallogr., Sect. A* **1990**, *46*, 467−473.
(18) Sheldrick, G. M. *SHELXL 97*, Program for crystal structure refinement; University of Göttingen: Göttingen, Germany, 1997.
(19) Clays, K.; Olbrechts, G.; Munters, T.; Persoons, A.; Kim O.-K.; Choi, L.-S. *Chem. Phys. Lett.* **1998**, *293*, 337−342.
(20) Olbrechts, G.; Strobbe, R.; Clays K.; Persoons, A. *Rev. Sci. Instrum*. **1998**, *69*, 2233−2241.
(21) Heesink, G. J. T.; Ruiter, A. G. T.; van Hulst, N. F.; Bölger, B. *Phys. Rev. Lett.* **1993**, *71*, 999−1002.
(22) Hendrickx, E.; Boutton, C.; Clays, K.; Persoons, A.; van Es, S.; Biemans, T.; Meijer, B. *Chem. Phys. Lett.* **1997**, *270*, 241−244.
(23) Boutton, C.; Clays, K.; Persoons, A.; Wada, T.; Sasabe, H. *Chem. Phys. Lett.* **1998**, *286*, 101−106.
(24) Shin, Y. K.; Brunschwig, B. S.; Creutz, C.; Sutin, N. *J. Phys. Chem.* **1996**, *100*, 8157−8169.
(25) Frisch, M. J. et al. *Gaussian 03*, revision B.05; Gaussian, Inc.: Pittsburgh, PA, 2003.
(26) The B3P86 Functional consists of Becke's three parameter hybrid functional (Becke, A. D. *J. Chem. Phys*. **1993**, *98*, 5648−5652) with the nonlocal correlation provided by the Perdew 86 expression: Perdew, J. P. *Phys. Rev. B* **1986**, *33*, 8822−8824.
(27) D95 on first row: Dunning, T. H.; Hay P. J. In *Modern Theoretical Chemistry*; Schaefer, H. F. III, Ed.; Plenum: New York, 1976, Vol. 3, p 1. Los Alamos ECP plus DZ on Na−Bi: (a) Hay, P. J.; Wadt, W. R. *J. Chem. Phys*. **1985**, *82*, 270−283. (b) Wadt, W. R.; Hay, P. J. *J. Chem. Phys*. **1985**, *82*, 284−298. (c) Hay, P. J.; Wadt, W. R. *J. Chem. Phys*. **1985**, *82*, 299−310.

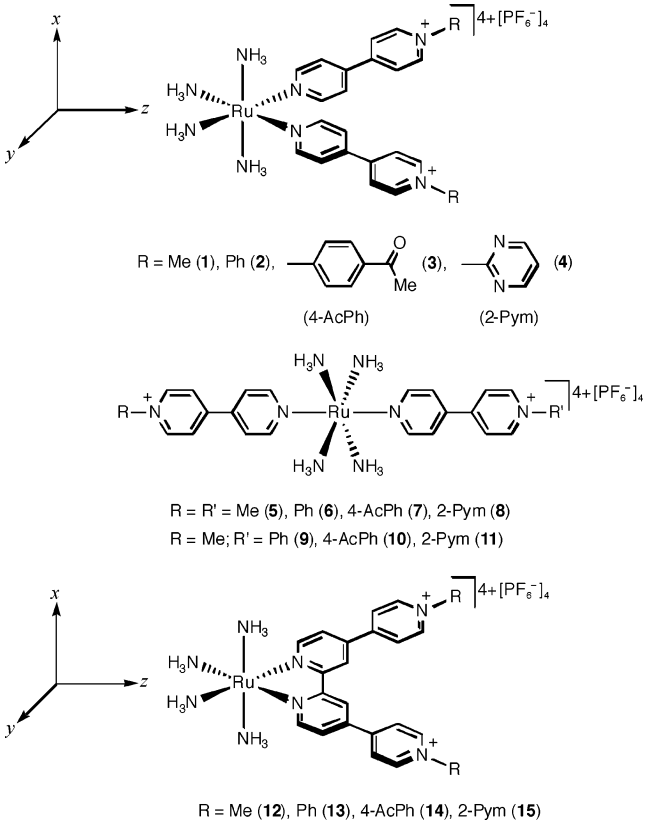

Figure 1. Chemical structures of the complex salts investigated, showing the axis convention used in the theoretical calculations.

programs use the so-called "standard orientation" that for a C_{2v} group assigns the *z* axis to the C_2 axis of symmetry and the molecule is placed on the *zy* plane with the *x* axis orthogonal to the molecule (as shown in Figure 1). The same model chemistry was used for properties calculations. Electronic transitions were calculated by means of the TD-DFT method, and the excited-state dipole moments were calculated by using the one particle RhoCI density. The default Gaussian 03 parameters were used in every case. Molecular orbital contours were plotted by using Molekel 4.3.[28]

Results and Discussion

Synthetic Studies. The compound 2,2′:4,4″:4′,4‴-quaterpyridyl (Qpy) was obtained by a modification of a literature method which involves heating at 125 °C for 72 h with 10% Pd on charcoal.[12] We have found that heating a 4,4′-bipyridyl (4,4′-bpy) melt at ca. 250 °C for 48 h with the same coupling reagent results in an approximately 30% increase in the yield of Qpy when compared with the published procedure,[12] and some higher-order oligopyridine byproducts are also generated. Qpy [also known as 4-(4-pyridyl)-2,2′:4′,4″-terpyridyl] has also been prepared in 26% yield via reaction of 4,4′-bpy with lithium diisopropylamide as the coupling reagent in diethyl ether at −78 °C, with subsequent warming to room temperature.[29] The new Qpy-based pro-ligand salts, $[R_2Qpy^{2+}][PF_6]_2$, (R = Ph, 4-AcPh or 2-Pym) were synthesized by using methods which we have previously developed to prepare analogous 4,4′-bpy-based ligands (Scheme 1).[5c,d] The compound $[(2,4\text{-DNPh})_2Qpy^{2+}]Cl_2$ (2,4-DNPh = 2,4-dinitrophenyl) was prepared as an intermediate, but not purified or characterized.

The new complex salts **1**−**15** (Figure 1) were prepared by using slight modifications of established coordination chemistry procedures based on the precursors *cis*-$[Ru^{III}Cl_2(NH_3)_4]Cl$,[10] *trans*-$[Ru^{II}Cl(NH_3)_4(SO_2)]Cl$,[11] or $[Ru^{II}(NH_3)_5(H_2O)][PF_6]_2$.[11] Five equivalents of the pro-ligand salts were used in the preparations of **1**−**4**, the unreacted excesses being readily separated by precipitation of the crude products from aqueous solutions with acetone. In contrast, only one equivalent of the required pro-ligand salt was used in the preparations of **12**−**15** because these reactions are relatively inefficient and substantial amounts of unreacted pro-ligand salt remain. Purification of **12**−**15**, largely involving removal of the unreacted pro-ligand salts, also proved rather more demanding than was the case for **1**−**11**. Two methods were adopted, one involving cycles of oxidation and reduction in which the remaining pro-ligand is converted into a relatively insoluble *N*-oxide, and the other using column chromatography on silica gel. Although both methods were attempted in each case, those described above gave the highest purified yields.

Electronic Spectroscopy Studies. Electronic absorption spectra for the new complex salts **1**−**15** were recorded in acetonitrile, and the results are presented in Table 1. As expected, all of the complexes show intense $d(Ru^{II}) \rightarrow \pi^*(L)$ (L = pyridinium ligand) metal-to-ligand charge-transfer (MLCT) bands in the visible region, together with UV bands due to intraligand $\pi \rightarrow \pi^*$ excitations.

Salts **1**−**4** each show two very close MLCT bands (Table 1, Figure 2), as found in other related complexes such as *cis*-$[Ru^{II}(NH_3)_4(L^1)_2]^{2+}$ [L^1 = pyridine (py), isonicotinamide (isn)].[30] A simple MO analysis has attributed these bands to orthogonally polarized excitations from primarily the HOMO (a 4d Ru orbital in the plane defined by the Ru−N(pyridyl) bonds) into two L-based LUMOs which are combinations of π^* MOs of the individual pyridyl ligands.[30b] Note, however, that in these previous studies the *x* and *y* axes were taken as lying along the Ru−N(pyridyl) bonds, with the *z* axis along the two mutually trans Ru−NH_3 bonds.[30b] Here we use a different axis labeling convention, as defined by the computational procedure and shown in Figure 1. For **1**−**4**, the lower-energy absorption is more intense than the higher-energy band in all cases, and the energy gap between these bands is constant at ca. 0.3 eV. As observed previously in related 1D complexes,[5d] the E_{max} values for both MLCT bands decrease as L changes in the order $MeQ^+ > PhQ^+ > 4\text{-}AcPhQ^+ > 2\text{-}PymQ^+$, due to the steadily increasing acceptor strength of the pyridinium groups. Simple MO theory also predicts that symmetric trans complexes such as those found in **5**−**8** should exhibit two MLCT transitions, but the higher-energy one is parity forbidden.[30b] This is consistent with the observed spectra, which again show the trend of decreasing E_{max} as the pyridinium groups become more electron deficient. The asymmetric trans complexes in **9**−**11** would be expected to show two close MLCT bands, those at higher energy corresponding to $d(Ru^{II}) \rightarrow \pi^*(MeQ^+)$ processes, but these bands are unsurprisingly not resolved in the spectra obtained.

(28) Portmann, S.; Lüthi, H. P. *Chimia* **2000**, *54*, 766−770.
(29) Hayes, M. A.; Meckel, C.; Schatz E.; Ward, M. D. *J. Chem. Soc., Dalton Trans.* **1992**, 703−708.
(30) (a) Ford P. C.; Sutton, C. *Inorg. Chem.* **1969**, *8*, 1544−1546. (b) Zwickel A. M.; Creutz, C. *Inorg. Chem.* **1971**, *10*, 2395−2399. (c) Pavanin, L. A.; Giesbrecht E.; Tfouni, E. *Inorg. Chem.* **1985**, *24*, 4444−4446. (d) Pavanin, L. A.; Novais da Rocha, Z.; Giesbrecht E.; Tfouni, E. *Inorg. Chem.* **1991**, *30*, 2185−2190.

Scheme 1. Syntheses of the Qpy-Based Pro-Ligands

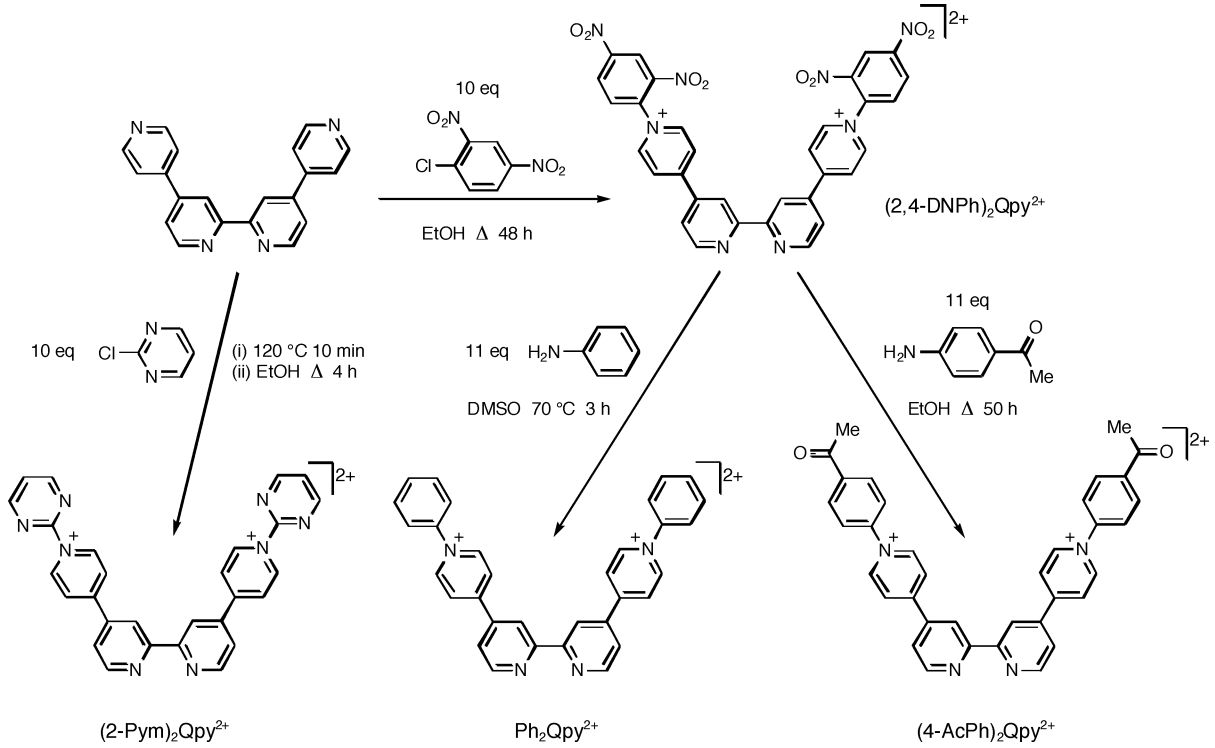

Table 1. UV−Visible Data for Complex Salts **1**−**15** in Acetonitrile[a]

salt	λ_{max}, nm (ϵ, M^{-1} cm^{-1})	E_{max} (eV)	assignment
1 *cis*-$[Ru^{II}(NH_3)_4(MeQ^+)_2][PF_6]_4$	570 (17 500)	2.18	d → π*
	502 (15 100)	2.47	d → π*
	262 (33 300)	4.73	π → π*
2 *cis*-$[Ru^{II}(NH_3)_4(PhQ^+)_2][PF_6]_4$	606 (20 400)	2.05	d → π*
	528 (16 500)	2.35	d → π*
	284 (31 200)	4.37	π → π*
3 *cis*-$[Ru^{II}(NH_3)_4(4\text{-}AcPhQ^+)_2][PF_6]_4$	620 (22 600)	2.00	d → π*
	536 (17 500)	2.31	d → π*
	288 (41 800)	4.31	π → π*
4 *cis*-$[Ru^{II}(NH_3)_4(2\text{-}PymQ^+)_2][PF_6]_4$	644 (21 500)	1.93	d → π*
	558 (17 200)	2.22	d → π*
	286 (44 600)	4.34	π → π*
5 *trans*-$[Ru^{II}(NH_3)_4(MeQ^+)_2][PF_6]_4$	595 (27 700)	2.08	d → π*
	259 (35 200)	4.79	π → π*
6 *trans*-$[Ru^{II}(NH_3)_4(PhQ^+)_2][PF_6]_4$	628 (29 400)	1.97	d → π*
	277 (31 700)	4.48	π → π*
7 *trans*-$[Ru^{II}(NH_3)_4(4\text{-}AcPhQ^+)_2][PF_6]_4$	641 (31 100)	1.93	d → π*
	283 (43 600)	4.38	π → π*
8 *trans*-$[Ru^{II}(NH_3)_4(2\text{-}PymQ^+)_2][PF_6]_4$	673 (33 700)	1.84	d → π*
	282 (53 500)	4.40	π → π*
9 *trans*-$[Ru^{II}(NH_3)_4(MeQ^+)(PhQ^+)][PF_6]_4$	611 (29 600)	2.03	d → π*
	268 (31 700)	4.63	π → π*
10 *trans*-$[Ru^{II}(NH_3)_4(MeQ^+)(4\text{-}AcPhQ^+)][PF_6]_4$	620 (30 700)	2.00	d → π*
	269 (35 800)	4.61	π → π*
11 *trans*-$[Ru^{II}(NH_3)_4(MeQ^+)(2\text{-}PymQ^+)][PF_6]_4$	639 (28 400)	1.94	d → π*
	272 (38 900)	4.56	π → π*
12 $[Ru^{II}(NH_3)_4(Me_2Qpy^{2+})][PF_6]_4$	510 (13 000)	2.43	d → π*
	320 (12 300)	3.88	π → π*
	260 (35 300)	4.77	π → π*
13 $[Ru^{II}(NH_3)_4(Ph_2Qpy^{2+})][PF_6]_4$	540 (25 000)	2.30	d → π*
	264 (35 500)	4.70	π → π*
14 $[Ru^{II}(NH_3)_4\{(4\text{-}AcPh)_2Qpy^{2+}\}][PF_6]_4$	548 (26 900)	2.26	d → π*
	288 (42 700)	4.31	π → π*
15 $[Ru^{II}(NH_3)_4\{(2\text{-}Pym)_2Qpy^{2+}\}][PF_6]_4$	568 (24 800)	2.18	d → π*
	286 (44 100)	4.34	π → π*

[a] Solutions ca. $3-8 \times 10^{-5}$ M.

The complex *cis*-$[Ru^{II}(NH_3)_4(2,2'\text{-bpy})]^{2+}$ (bpy = bipyridyl) was first reported in 1974,[31] and quite a number of studies into its electronic structure have since been carried out.[32] This species has two MLCT bands, with λ_{max} values of 526 and 365 nm (for the PF_6^- salt in acetonitrile),[32c] and INDO/S calculations predict a number of closely spaced transitions, polarized in the bpy

Table 2. Electrochemical Data for Complex Salts **1**−**15** and $[Me_2Qpy^{2+}][PF_6]_2$ in Acetonitrile

	$E_{1/2}$, V vs Ag–AgCl (ΔE_p, mV)[a]			E (V vs Ag–AgCl)[a,b]	
salt	$Ru^{III/II}$	$L^{+/0}/L^{2+/0}$	$L^{0/-}/L^{-/2-}/L^{0/2-}$	$L^{+/0}/L^{2+/+}$	$L^{0/-}/L^{-/2-}$
1 *cis*-$[Ru^{II}(NH_3)_4(MeQ^+)_2][PF_6]_4$	0.79 (85)	−0.81 (110)	−1.42 (65)	−0.79	−1.40
			−1.55 (70)		−1.54
2 *cis*-$[Ru^{II}(NH_3)_4(PhQ^+)_2][PF_6]_4$	0.79 (70)	−0.66 (110)	−1.26 (70)	−0.64	−1.23
			−1.38 (65)		−1.36
3 *cis*-$[Ru^{II}(NH_3)_4(4\text{-}AcPhQ^+)_2][PF_6]_4$	0.80 (70)	−0.55 (120)	−1.09 (290)[c]		
4 *cis*-$[Ru^{II}(NH_3)_4(2\text{-}PymQ^+)_2][PF_6]_4$	0.82 (100)	−0.42[d]			
5 *trans*-$[Ru^{II}(NH_3)_4(MeQ^+)_2][PF_6]_4$	0.74 (100)	−0.83 (130)	−1.38[d]		
			−1.45[d]		
6 *trans*-$[Ru^{II}(NH_3)_4(PhQ^+)_2][PF_6]_4$	0.76 (90)	−0.66 (100)	−1.21[d]		
			−1.25[d]		
			−1.36[d]		
7 *trans*-$[Ru^{II}(NH_3)_4(4\text{-}AcPhQ^+)_2][PF_6]_4$	0.77 (90)	−0.56 (100)	−1.09[d]		
8 *trans*-$[Ru^{II}(NH_3)_4(2\text{-}PymQ^+)_2][PF_6]_4$	0.76 (80)	−0.44[d]			
9 *trans*-$[Ru^{II}(NH_3)_4(MeQ^+)(PhQ^+)][PF_6]_4$	0.72 (100)	−0.66 (70)	−1.27 (80)		
		−0.86 (70)			
10 *trans*-$[Ru^{II}(NH_3)_4(MeQ^+)(4\text{-}AcPhQ^+)][PF_6]_4$	0.74 (90)	−0.58 (80)	−1.11 (150)		
		−0.84 (80)			
11 *trans*-$[Ru^{II}(NH_3)_4(MeQ^+)(2\text{-}PymQ^+)][PF_6]_4$	0.74 (90)	−0.41 (90)	−1.16 (100)		
		−0.85 (70)			
12 $[Ru^{II}(NH_3)_4(Me_2Qpy^{2+})][PF_6]_4$	0.79 (85)	−0.82 (160)	−1.39 (80)	−0.74	−1.37
			−1.61 (95)	−0.84	−1.57
13 $[Ru^{II}(NH_3)_4(Ph_2Qpy^{2+})][PF_6]_4$	0.81 (90)	−0.64 (130)	−1.21 (75)	−0.55	−1.19
			−1.40 (70)	−0.65	−1.38[e]
14 $[Ru^{II}(NH_3)_4\{(4\text{-}AcPh)_2Qpy^{2+}\}][PF_6]_4$	0.82 (70)	−0.56[d]			
15 $[Ru^{II}(NH_3)_4\{(2\text{-}Pym)_2Qpy^{2+}\}][PF_6]_4$	0.83 (80)	−0.37[d]			
$[Me_2Qpy^{2+}][PF_6]_2$		−0.91 (110)	−1.57 (85)		

[a] Measured in solutions ca. 10^{-3} M in analyte and 0.1 M in $[NBu^n_4]PF_6$ at a platinum bead/disk working electrode with a scan rate of 200 mV s^{-1}. Ferrocene internal reference $E_{1/2}$ = 0.44 V, ΔE_p = 70 mV. [b] Potential increment = 4 mV, amplitude = 50 mV, pulse width = 0.05 s. [c] Shoulders evident. [d] E_{pc} for an irreversible reduction process. [e] Potential increment = 1 mV.

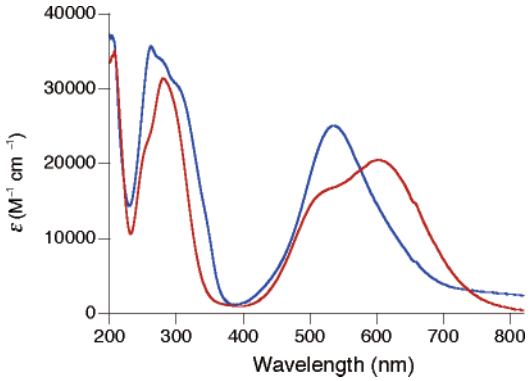

Figure 2. UV−visible absorption spectra of **2** (red) and **13** (blue) at 295 K in acetonitrile.

plane, as well as weak perpendicularly polarized nonbonding d → π^* transitions.[32b] The related complexes in **12**−**15** exhibit only broad MLCT bands in the visible region which result from two or more transitions. In each case the absorption profile is asymmetrical, with a tail on the lower energy side indicating the presence of a less intense low energy transition. The absence of MLCT absorptions in the UV is consistent with stabilization of the ligand π^* orbitals when compared with those of 2,2′-bpy in *cis*-$[Ru^{II}(NH_3)_4(2,2'\text{-bpy})]^{2+}$. Representative UV−visible spectra of **2** and **13** are shown in Figure 2. As expected, the formation of a planar chelating system by linking the two coordinated 4,4′-bipyridinium units dramatically alters the electronic structures, and hence absorption spectra, of these *cis*-$\{Ru^{II}(NH_3)_4\}^{2+}$ complexes. However, the overall decreased extent of visible absorption (observed for example on moving from **2** to **13**) contrasts with the behavior of the simpler complexes *cis*-$[Ru^{II}(NH_3)_4(py)_2]^{2+}$ and *cis*-$[Ru^{II}(NH_3)_4(2,2'\text{-bpy})]^{2+}$. The former is yellow, with a lowest-energy MLCT band at λ_{max} = 409 nm (for the PF_6^- salt in acetonitrile),[33] while the latter displays a dark red-purple color.

Electrochemical Studies. The new complex salts **1**−**15** were studied by cyclic voltammetry in acetonitrile, and the results are presented in Table 2. All of the complexes show reversible or quasi-reversible $Ru^{III/II}$ oxidation waves, together with reversible, quasi-reversible, and/or irreversible ligand-based reduction processes. It is worth noting that such species exhibiting several reversible redox processes offer intriguing possibilities for multistate switching of NLO responses, exploiting not only $Ru^{III/II}$ oxidations[6] but also ligand-based reductions. Representative cyclic voltammograms of the salts **1** and **12** are shown in Figure 3.

Literature $Ru^{III/II}$ $E_{1/2}$ values for the salts *cis*-$[Ru^{II}(NH_3)_4(py)_2](PF_6)_2$[33] and *cis*-$[Ru^{II}(NH_3)_4(2,2'\text{-bpy})](PF_6)_2$[11] are respectively 0.54 and 0.53 V vs Ag−AgCl, ca. 200−300 mV lower than the corresponding potentials observed for **1**−**15**. It is therefore apparent that the electron-withdrawing influence of the two pyridinium substituents in the new complexes causes substantial stabilization of the Ru-based HOMOs when compared with the model compounds. The accompanying red-shifting of the MLCT bands in **1**−**15** (see above) is therefore indicative of very pronounced stabilization of the ligand-based LUMOs which more than offsets that of the HOMOs. As noted previously,[5c,d] the $Ru^{III/II}$ $E_{1/2}$ values of complexes of *N*-R-4,4′-bipyridinium

(31) Alvarez, V. E.; Allen, R. J.; Matsubara T.; Ford, P. C. *J. Am. Chem. Soc.* **1974**, *96*, 7686−7692.
(32) Selected examples: (a) Mines, G. A.; Roberts J. A.; Hupp, J. T. *Inorg. Chem.* **1992**, *31*, 125−128. (b) Streiff, J. H.; Edwards W. D.; McHale, J. L. *Chem. Phys. Lett.* **1999**, *312*, 369−375. (c) Endicott, J. F.; Schlegel, H. B.; Uddin Md. J.; Seniveratne, D. S. *Coord. Chem. Rev.* **2002**, *229*, 95−106.
(33) Ando, I.; Ishimura, D.; Ujimoto K.; Kurihara, H. *Inorg. Chem.* **1996**, *35*, 3504−3508.

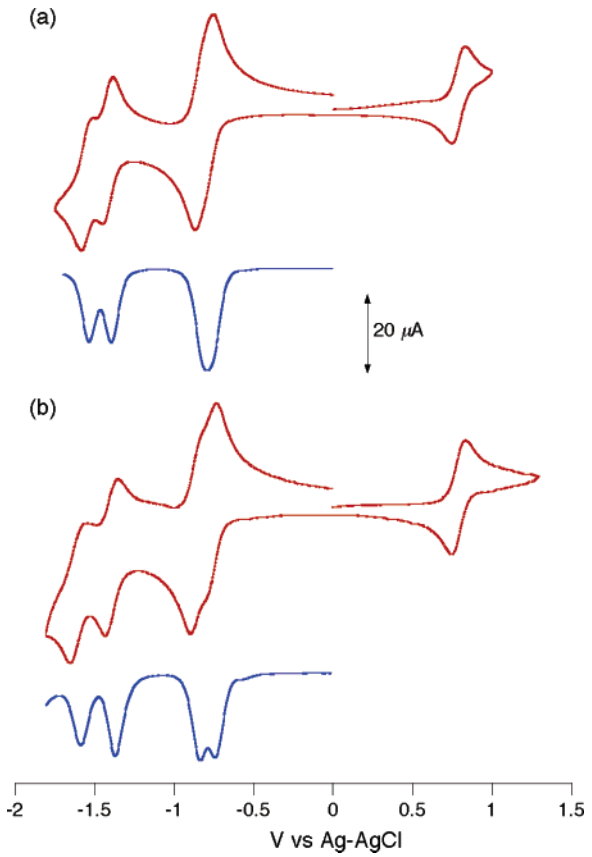

Figure 3. Cyclic (red) and differential pulse (blue) voltammograms of **1** (a) and **12** (b) in acetonitrile.

ligands are relatively insensitive to changes in R. However, within each of the three series **1**−**4**, **5**−**8**, and **12**−**15**, the $Ru^{III/II}$ $E_{1/2}$ increases slightly, as the HOMO becomes stabilized by the increasing electron-accepting ability of the pyridinium substituent. The $Ru^{III/II}$ potentials for the trans complex salts are a little lower (by 30−80 mV) than those of their cis analogues, but the latter and their Qpy-based counterparts have essentially identical $Ru^{III/II}$ $E_{1/2}$ values, showing that chelate formation does not significantly affect the HOMO energy.

The complexes in salts **4**, **8**, **14**, and **15** exhibit only one irreversible reduction process, but **1**−**3** show especially interesting ligand-based electrochemistry, with broad, quasi-reversible (presumably) two-electron $L^{+/0}$ reductions. The $E_{1/2}$ values of these waves increase as R changes in the order Me < Ph < 4-AcPh, reflecting the increasing acceptor strength of the 4,4′-bipyridinium ligands which is mirrored in the red-shifting of the MLCT bands. Similar first-ligand reduction waves are also seen in the salts **5**−**7** and **12** and **13**, but in the latter two compounds the two-electron $L^{2+/0}$ waves show slight shoulders, indicating two separate processes occurring at similar potentials. Differential pulse voltammetry experiments resolve these processes for **12** and **13**, but not for **1** and **2** (Table 2, Figure 3), showing that with the Qpy-based ligands there is a detectable degree of electronic communication between the pyridinium moieties. The absence of a direct linkage between the coordinated pyridyl rings logically results in a smaller extent of coupling in **1** and **2**.

Each of the cis complexes with *N*-Me and *N*-Ph substituents also shows two separate, reversible $L^{0/-}$ or $L^{-/2-}$ reduction processes with differences between the $E_{1/2}$ values of 130, 120, 220, and 190 mV for **1**, **2**, **12**, and **13**, respectively. These observations show that the extent of electronic coupling between the pyridyl ligands increases upon reduction, and the Qpy-based systems again show greater coupling compared with their nonchelated analogues. In contrast, the pro-ligand salt $[Me_2Qpy^{2+}][PF_6]_2$ exhibits only one broad reversible $Me_2Qpy^{2+/0}$ wave and one $Me_2Qpy^{0/2-}$ wave, showing that metal coordination is required to allow significant communication between the pyridinium groups. This is entirely logical because the 2,2′-bpy unit in Qpy derivatives would be expected to adopt a transoid geometry unless chelated, as confirmed by the crystal structure of $[Ph_2Qpy^{2+}][PF_6]_2{\cdot}Me_2CO$ (see Figure 4 and Table 3). All of the trans complexes show only irreversible or quasi-irreversible $L^{0/-}$ processes, with the exception of **9**.

Table 3. Crystallographic Data and Refinement Details for Salt $[Ph_2Qpy^{2+}][PF_6]_2{\cdot}Me_2CO$

formula	$C_{35}H_{30}F_{12}N_4OP_2$
M	812.57
crystal system	monoclinic
space group	*C*2/*c*
a/Å	24.1853(7)
b/Å	10.3325(3)
c/Å	14.4450(2)
β/deg	110.375(2)
U/Å^3	3383.88(15)
Z	4
T/K	120(2)
μ/mm^{-1}	0.233
reflections collected	19666
independent reflections (R_{int})	3742 (0.0795)
final R1, wR2 [$I > 2\sigma(I)$][a]	0.0405, 0.1044
(all data)	0.0528, 0.1124

[a] The structure was refined on F_o^2 using all data; the value of R1 is given for comparison with older refinements based on F_o with a typical threshold of $F_o > 4\sigma(F_o)$.

Crystallographic Study. A single-crystal X-ray structure was obtained for the pro-ligand salt $[Ph_2Qpy^{2+}][PF_6]_2{\cdot}Me_2CO$. A representation of the molecular structure of this salt is shown in Figure 4, and selected interatomic distances and angles are presented in Table 4. To our knowledge, this is the first reported structure of a compound containing a Qpy unit.

As expected, the 2,2′-bpy unit in $[Ph_2Qpy^{2+}][PF_6]_2{\cdot}Me_2CO$ adopts a planar, transoid geometry to minimize steric repulsions, with a center of symmetry in the middle of the C−C bond between the pyridyl rings. The structure is otherwise heavily twisted, with dihedral angles of 34.65° between the two 4-pyridyl rings and 49.35° between the pyridyl and attached phenyl rings.

Hyper-Rayleigh Scattering Studies. The β values of **1**−**4** and **12**−**15** were measured in acetone solutions by using the HRS technique[7,19,20] with an 800 nm Ti^{3+}:sapphire laser, and the results are collected in Table 5. This laser fundamental was chosen because none of the complexes absorb strongly at either 800 nm or at the second harmonic (SH) of 400 nm, their MLCT bands falling conveniently between these wavelengths (Figure 2). Other available laser fundamentals, such as 1064 or 1300 nm, would be unsuitable due to very strong absorption at their SH wavelengths. Using an 800 nm laser also has the advantage of avoiding any possibility of fluorescence contributions at the SH, which can cause problems in HRS studies.[20] **1**−**4** were also studied in acetonitrile. Because the symmetric trans complexes would be expected to possess β values of zero and their

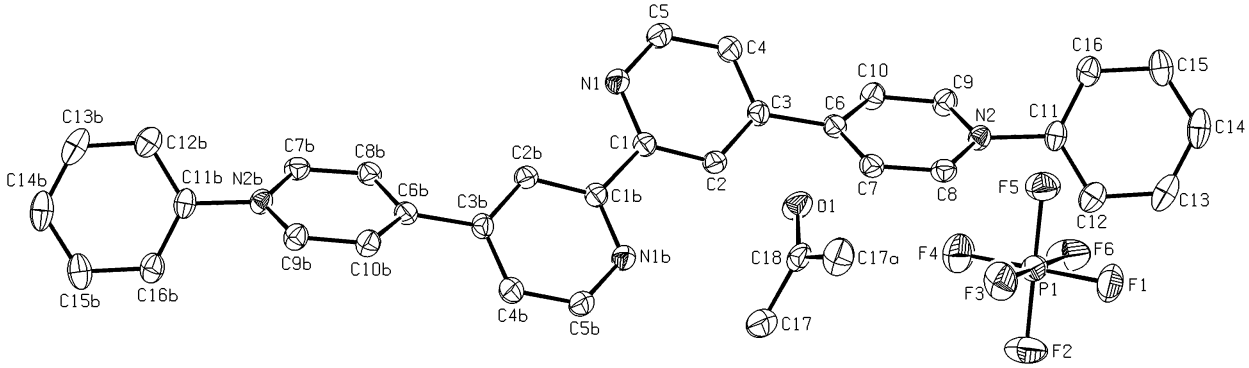

Figure 4. Representation of the molecular structure of the salt $[Ph_2Qpy^{2+}][PF_6]_2 \cdot Me_2CO$ (only one PF_6^- is shown because the asymmetric unit contains only half a PF_6^- and the drawing software therefore automatically generates only one ion).

Table 4. Selected Interatomic Distances (Å) and Angles (deg) for Salt $[Ph_2Qpy^{2+}][PF_6]_2 \cdot Me_2CO$[a]

C1−N1	1.343(2)	C6−C7	1.391(2)
C1−C2	1.395(2)	C6−C10	1.397(2)
C1−C1^{ii}	1.494(3)	C7−C8	1.374(2)
C2−C3	1.391(2)	C8−N2	1.353(2)
C3−C4	1.388(2)	C9−N2	1.347(2)
C3−C6	1.487(2)	C9−C10	1.379(2)
C4−C5	1.389(2)	C11−N2	1.454(2)
C5−N1	1.334(2)		
N1−C1−C2	122.95(14)	C12−C11−N2	119.47(15)
N1−C1−C1^{ii}	116.19(17)	C5−N1−C1	117.34(14)
N1−C5−C4	123.66(15)	C9−N2−C8	120.51(14)
N2−C8−C7	120.70(15)	C9−N2−C11	120.58(13)
N2−C9−C10	120.58(15)	C8−N2−C11	118.67(13)
C16−C11−N2	117.97(14)		

[a] Symmetry transformation used to generate equivalent atoms: (ii) −x,−y+1,−z+1.

Table 5. MLCT and HRS Data for Complex Salts **1**−**4** and **12**−**15**

	λ_{max}[MLCT] (nm)		β_{800}[a] (10^{-30} esu)	
salt	Me_2CO	MeCN	Me_2CO	MeCN
1 *cis*-$[Ru^{II}(NH_3)_4(MeQ^+)_2][PF_6]_4$	586	570	135	139
	508	502		
2 *cis*-$[Ru^{II}(NH_3)_4(PhQ^+)_2][PF_6]_4$	624	606	142	127
	536	528		
3 *cis*-$[Ru^{II}(NH_3)_4(4\text{-}AcPhQ^+)_2][PF_6]_4$	638	620	135	142
	540	536		
4 *cis*-$[Ru^{II}(NH_3)_4(2\text{-}PymQ^+)_2][PF_6]_4$	672	644	160	143
	568	558		
12 $[Ru^{II}(NH_3)_4(Me_2Qpy^{2+})][PF_6]_4$	514	510	32	−
13 $[Ru^{II}(NH_3)_4(Ph_2Qpy^{2+})][PF_6]_4$	544	540	48	−
14 $[Ru^{II}(NH_3)_4\{(4\text{-}AcPh)_2Qpy^{2+}\}][PF_6]_4$	552	548	40	−
15 $[Ru^{II}(NH_3)_4\{(2\text{-}Pym)_2Qpy^{2+}\}][PF_6]_4$	574	568	42	−

[a] First hyperpolarizability measured by using a 800 nm Ti^{3+}:sapphire laser fundamental (±15% error), assuming a single major tensor component. The quoted cgs units (esu) can be converted into SI units ($C^3\ m^3\ J^{-2}$) by dividing by a factor of 2.693×10^{20}.

asymmetric counterparts should display only small responses, **5**−**11** were not investigated via HRS.

The following conclusions can be drawn from the data in Table 5: (i) the β_{800} values for **1**−**4** are all similar and do not show a significant variation in the two solvents chosen, and (ii) the β_{800} values for **12**−**15** are also similar, but substantially smaller than those of their nonchelated counterparts **1**−**4**. In our previous studies with related 1D dipolar complex chromophores of *N*-R-4,4′-bipyridinium ligands, we have noted that substantial increases in β_0 (the estimated static first hyperpolarizability) are observed on changing R from a Me to an aryl substituent.[5b−d] Although the data in acetone may indicate

Table 6. HRS Depolarization Ratios and β Components for Complex Salts **1**−**4**

salt	ρ[a]	k	β_{zzz}[b] (10^{-30} esu)	β_{zyy}[c] (10^{-30} esu)
1 *cis*-$[Ru^{II}(NH_3)_4(MeQ^+)_2][PF_6]_4$	2.32 ± 0.05	−0.36	142	−51
2 *cis*-$[Ru^{II}(NH_3)_4(PhQ^+)_2][PF_6]_4$	2.07 ± 0.06	−0.43	126	−54
3 *cis*-$[Ru^{II}(NH_3)_4(4\text{-}AcPhQ^+)_2][PF_6]_4$	2.09 ± 0.05	−0.43	141	−61
4 *cis*-$[Ru^{II}(NH_3)_4(2\text{-}PymQ^+)_2][PF_6]_4$	2.11 ± 0.06	−0.42	143	−60

[a] Depolarization ratio determined in acetonitrile by using a 800 nm Ti^{3+}:sapphire laser fundamental. [b,c] Hyperpolarizability tensor components derived from the HRS intensity and depolarization ratio measurements by using eqs 8−10.

a small degree of enhancement of β_{800} for the complexes of *N*-aryl ligands when compared with their *N*-Me analogues, the data for **1**−**4** in acetonitrile do not reinforce this putative trend.

Although the β_{800} data given in Table 5 are based on the assumption of a single β component, the hyperpolarizabilities of **1**−**4** and **12**−**15** are expected to display substantial 2D character. For a chromophore with C_{2v} symmetry, there are five nonzero components of the β tensor, β_{zzz}, β_{zyy}, β_{zxx}, β_{yyz}, and β_{xxz}. Assuming Kleinman symmetry, $\beta_{zyy} = \beta_{yyz}$ and $\beta_{zxx} = \beta_{xxz}$. Furthermore, if we assume an essentially 2D structure, then $\beta_{zxx} = \beta_{xxz} = 0$. Hence, only the components β_{zzz} and β_{zyy} are significant. The lack of existing NLO chromophores structurally similar to **1**−**4** and **12**−**15** renders comparisons with published cases difficult. In previous HRS studies on the complex *fac*-$Re^{I}Br(CO)_3(L^2)_2$ [L^2 = *trans*-4-(4-(dimethylamino)-phenyl-4-buta-1,3-dienyl)pyridine] it was assumed that the chromophore consists of two noninteracting 1D dipolar subunits, separated by an angle of 90°.[4d] In such a case, β_{zzz} and β_{zyy} are equal. A similar approach has been applied to neutral, purely organic C_{2v} chromophores.[22,23] However, the observation of multiple MLCT bands clearly shows that to treat the cations in **1**−**4** and **12**−**15** as containing noninteracting 1D dipolar subunits is rather an oversimplification. Hence, to obtain further information about the importance of off-diagonal tensor components in these chromophores, we have measured HRS depolarization ratios ρ for **1**−**4** (Table 6). The quantity ρ is defined as the ratio of the intensities of the scattered SH light polarized parallel and perpendicular to the polarization direction of the fundamental light.[21] Unfortunately, the relatively low harmonic scattering intensities for **12**−**15** preclude the determination of ρ values for these compounds.

A ρ value of 5 is the upper limit for purely dipolar symmetry, i.e. a single dipolar β tensor component or for C_{2v} symmetry with identical β_{zzz} and β_{zyy} tensor components, and in the limit of ideal experimental conditions, while a ρ of 1.5 is the lower

Table 7. Visible Absorption and Stark Spectroscopic Data for Complex Salts **1**−**4** and **12**−**15**[a]

salt	λ_{max}[b] (nm)	E_{max}[b] (eV)	f_{os}[b]	μ_{12}[c] (D)	$\Delta\mu_{12}$[d] (D)	$\Delta\mu_{ab}$[e] (D)	r_{12}[f] (Å)	r_{ab}[g] (Å)	c_b^2[h]	H_{ab}[i] (cm^{-1})	β_0[j] (10^{-30} esu)
1 *cis*-$[Ru^{II}(NH_3)_4(MeQ^+)_2][PF_6]_4$[k]	628	1.98	0.34	6.7	10.1	16.8	2.1	3.5	0.20	6400	137
	518	2.39	0.24	5.2	11.3	15.3	2.4	3.2	0.13	6500	62
2 *cis*-$[Ru^{II}(NH_3)_4(PhQ^+)_2][PF_6]_4$[k]	632	1.96	0.41	7.4	13.8	20.3	2.9	4.2	0.16	5800	231
	512	2.42	0.20	4.6	9.9	13.5	2.1	2.8	0.13	6700	42
3 *cis*-$[Ru^{II}(NH_3)_4(4\text{-}AcPhQ^+)_2][PF_6]_4$[k]	684	1.81	0.40	7.6	12.1	19.5	2.5	4.1	0.19	5700	248
	558	2.22	0.26	5.6	13.0	17.1	2.7	3.6	0.12	5800	95
4 *cis*-$[Ru^{II}(NH_3)_4(2\text{-}PymQ^+)_2][PF_6]_4$[k]	731	1.97	0.40	7.9	11.7	19.7	2.4	4.1	0.20	5500	298
	589	2.10	0.27	5.9	12.3	16.9	2.6	3.5	0.14	5900	110
12 $[Ru^{II}(NH_3)_4(Me_2Qpy^{2+})][PF_6]_4$	547	2.27	0.18	4.5	13.0	15.8	2.7	3.3	0.09	5200	60
	497	2.49	0.20	4.6	18.4	20.5	3.9	4.4	0.05	4500	72
13 $[Ru^{II}(NH_3)_4(Ph_2Qpy^{2+})][PF_6]_4$	570	2.17	0.22	5.2	12.9	16.6	2.7	3.5	0.11	5500	86
14 $[Ru^{II}(NH_3)_4\{(4\text{-}AcPh)_2Qpy^{2+}\}][PF_6]_4$	581	2.13	0.24	5.4	12.9	16.9	2.7	3.5	0.12	5500	97
15 $[Ru^{II}(NH_3)_4\{(2\text{-}Pym)_2Qpy^{2+}\}][PF_6]_4$	608	2.04	0.26	5.8	12.9	17.3	2.7	3.6	0.13	5500	120

[a] Measured in butyronitrile glasses at 77 K. [b] For the two fitted Gaussian components. [c] Calculated from eq 4. [d] Calculated from $f_{int}\Delta\mu_{12}$ using $f_{int} = 1.33$. [e] Calculated from eq 3. [f] Delocalized electron-transfer distance calculated from $\Delta\mu_{12}/e$. [g] Effective (localized) electron-transfer distance calculated from $\Delta\mu_{ab}/e$. [h] Calculated from eq 5. [i] Calculated from eq 6. [j] Calculated from eq 7. [k] Data taken in part from ref 9.

limit for complete octopolar symmetry. The value of 3.4 determined for the reference compound Disperse Red 1 (DR1) is a good indication of a single major tensor component in DR1 and an appropriate experimental setup. The low ρ values obtained for **1**−**4** clearly indicate that the hyperpolarizabilities of these chromophores have substantial 2D character, and as with the MLCT spectra, are not consistent with the presence of two noninteracting chromophores. The values of β_{zzz} and β_{zyy} can be experimentally determined from two observables, the total HRS intensity $\langle\beta^2_{HRS}\rangle$ and ρ as follows:

$$\begin{cases}\langle\beta^2_{HRS}\rangle = \langle\beta^2_{ZZZ}\rangle + \langle\beta^2_{YZZ}\rangle \\ \rho = \dfrac{\langle\beta^2_{ZZZ}\rangle}{\langle\beta^2_{YZZ}\rangle}\end{cases} \tag{8}$$

The HRS intensity with parallel polarization for fundamental and SH wavelength, $\langle\beta^2_{ZZZ}\rangle$, and for perpendicular polarization, $\langle\beta^2_{YZZ}\rangle$, are given in terms of the molecular tensor components β_{zzz} and β_{zyy} according to

$$\begin{cases}\langle\beta^2_{ZZZ}\rangle = \dfrac{1}{7}\beta^2_{zzz} + \dfrac{6}{35}\beta_{zzz}\beta_{zyy} + \dfrac{9}{35}\beta^2_{zyy} \\ \langle\beta^2_{YZZ}\rangle = \dfrac{1}{35}\beta^2_{zzz} - \dfrac{2}{105}\beta_{zzz}\beta_{zyy} + \dfrac{11}{105}\beta^2_{zyy}\end{cases} \tag{9}$$

and ρ can be expressed in terms of the parameter $k = \beta_{zyy}/\beta_{zzz}$ by

$$\rho = \frac{15 + 18k + 27k^2}{3 - 2k + 11k^2} \tag{10}$$

Application of eqs 8−10 to our experimental data in acetonitrile affords the β_{zzz} and β_{zyy} values shown in Table 6. These data, when compared with those in Table 5, show that ρ is a very sensitive function of off-diagonal tensor components and confirm the 2D nature of the molecular NLO responses of **1**−**4**.

Stark Spectroscopic Studies. Complex salts **1**−**4** and **12**−**15** were studied by Stark spectroscopy[8] in butyronitrile glasses at 77 K, and the results are presented in Table 7. Unsurprisingly, Gaussian-fitting of the absorption spectra was necessary to successfully model the Stark data, using two or three curves in each case. For **1**−**4** and **12**, two of these curves contributed the majority of the Stark signal, but in **13**−**15** only one of the curves contributed most of the signal, and thus the data yielded by the insignificant curves have been neglected. Although the absorption profiles for **13**−**15** do indicate the presence of two MLCT bands, the Stark fitting approach does not allow fits with two reasonable Gaussian curves in these cases. The fitting invariably affords one large Gaussian with a reasonable $\Delta\mu_{12}$ (as given in Table 7) and one small but very wide Gaussian with an unrealistically large $\Delta\mu_{12}$ for the types of complex chromophore under study. For example, the data obtained for the small curve in **14** gives a $\Delta\mu_{12}$ of 7.42 eÅ or 35 D. Note that the $\Delta\mu_{12}$ quoted for the second band in **12** (18.4 D) is also relatively large, but perhaps not implausible. The Stark results for **1**−**4** are therefore probably more reliable than those for **12**−**15**. Gaussian-fitting has previously been adopted in Stark analyses of purely organic[34] and metal-containing chromophores,[35] but has only rarely been used to derive NLO responses.[36] Representative absorption spectra and electroabsorption spectra for the salts **1** and **14** are shown in Figure 5.

As observed previously in related compounds,[5e,24] the MLCT bands of **1**−**4** and **12**−**15** undergo large red-shifts when moving from 295 K acetonitrile solution to a 77 K butyronitrile glass (Tables 1 and 7). No clear trends are observed in the μ_{12} or $\Delta\mu_{12}$ values, but the $\Delta\mu_{ab}$ values are considerably larger than their adiabatic counterparts, as also observed in related compounds.[5e,24] The magnitudes of c_b^2 and H_{ab} found for **1**−**4** and **12**−**15** are similar to those for related complex chromophores,[5e,24] and are consistent with the assignment of the visible absorptions as arising from MLCT transitions in which the degree of delocalization is limited. For the Qpy-based chromophores in **12**−**15**, this conclusion contrasts with the results of previous electrochemical[32a] and vibrational spectroscopic[32a,c] studies which indicate substantial ground-state charge delocalization in the parent complex *cis*-$[Ru^{II}(NH_3)_4(2,2'\text{-bpy})]^{2+}$. However, as noted earlier, it is apparent that introduction of

(34) Bublitz, G. U.; Ortiz, R.; Marder S. R.; Boxer, S. G. *J. Am. Chem. Soc.* **1997**, *119*, 3365−3376.
(35) (a) Karki L.; Hupp, J. T. *Inorg. Chem.* **1997**, *36*, 3318−3321. (b) Karki, L.; Williams, R. D.; Hupp, J. T.; Allan, C. B.; Spreer, L. O. *Inorg. Chem.* **1998**, *37*, 2837−2840. (c) Bublitz, G. U.; Laidlaw, W. M.; Denning R. G.; Boxer, S. G. *J. Am. Chem. Soc.* **1998**, *120*, 6068−6075. (d) Walters, K. A.; Premvardhan, L. L.; Liu, Y.; Peteanu L. A.; Schanze, K. S. *Chem. Phys. Lett.* **2001**, *339*, 255−262.
(36) Vance F. W.; Hupp, J. T. *J. Am. Chem. Soc.* **1999**, *121*, 4047−4053. Note, however, that in this case the chromophore is a 3D pseudo-octopolar derivative of $[Ru^{II}(2,2'\text{-bpy})_3]^{2+}$ which has a complex electronic structure in which β is dominated by intra-ligand CT, rather than MLCT processes.

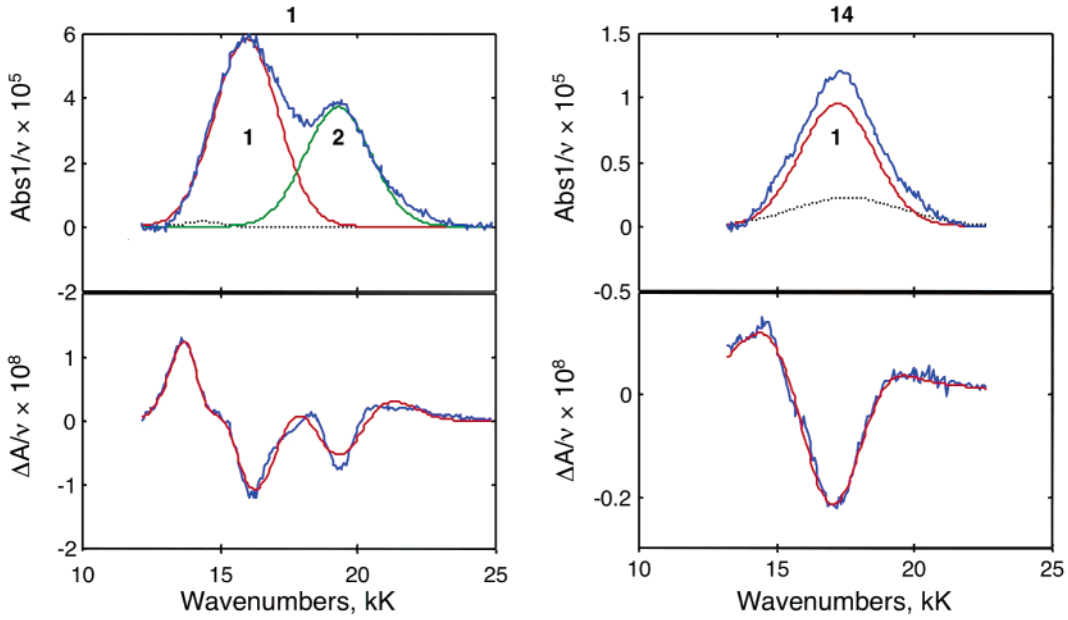

Figure 5. Stark spectra and calculated fits for **1** and **14** in external electric fields of 3.26 and 2.79 × 10^7 V m^{-1}, respectively. (Top) Absorption spectrum illustrating Gaussian curves utilized in data fitting (numbers signify components which contribute significantly to the Stark signal; the data for which are reported). (Bottom) Electroabsorption spectrum, experimental (blue) and fits (red) according to eq 1.

the 4-pyridinium substituents at the 4,4′-positions of the bpy ligand markedly alters the overall electronic structures of these complexes.

Although it is likely that application of the traditional two-state model to the electronic transitions of **1**−**4** and **12**−**15** is somewhat of an approximation,[3g,k] such a simplified approach has been applied previously to purely organic C_{2v} dipolar chromophores, giving reasonable results.[3a,d,f,j] We have therefore used eq 7 to estimate the magnitudes of the two orthogonal β_0 components for our complexes (Table 7).[37] As expected, the results show that the molecular quadratic NLO responses of **1**−**4** and **12** have considerable 2D nature, in agreement with the HRS data for **1**−**4**. It is notable that the β_0 values quoted in Table 7 compare favorably with most of those previously reported for C_{2v} dipolar organic chromophores[3a,d−l] and neutral metal complexes,[2l,4] and are by no means yet optimized. Comparison of the present results with the data available for the related 1D complexes $[Ru^{II}(NH_3)_5L]^{3+}$ [L(β_0 × 10^{30} esu): MeQ^+ (120); PhQ^+ (186); 4-$AcPhQ^+$ (229)][5e] affords the following general conclusions: (i) the β_0 values for both types of chromophore are similarly large, and (ii) *N*-arylation causes substantial increases in β_0 when compared with the MeQ^+ complexes in both 1D and 2D cases (although the data for **2** are perhaps anomalous).

Broadly speaking, these Stark-derived β_0 values are consistent with the HRS β_{800} data (Table 5) inasmuch as the NLO responses of the nonchelated chromophores are found to be larger than those of their Qpy-based analogues. Furthermore, the derivation of two substantial β components for **1**−**4** via both techniques (Tables 6 and 7) verifies the 2D nature of the NLO responses. However, any more detailed comparisons between the two sets of data should be made only with caution. While the Stark analysis indirectly affords estimated directional components of β associated with the MLCT transitions, the HRS measurements are direct but a function of all nonzero tensor components. Furthermore, the Stark and HRS experiments are carried out under quite different physical conditions of medium and temperature, which may affect the molecular NLO properties. Regarding the magnitudes of the observed β responses for **1**−**4** and **12**−**15**, a factor which can be expected to limit these is the decreased electron-donating strength of the Ru^{II} centers, as evidenced by their $Ru^{III/II}$ $E_{1/2}$ values of ca. 0.80 V vs Ag−AgCl, which are ca. 300 mV higher than those of their previously studied $[Ru^{II}(NH_3)_5L]^{3+}$ analogues.[5c,d]

Theoretical Studies. To shed further light on the molecular electronic structures of **1**−**4** and **12**−**15**, we have performed theoretical calculations on the representative model complex chromophores in salts **1** and **12** using Gaussian 03. The geometries were optimized at the B3P86/LanL2DZ model chemistry, and both Finite Field (FF) and TD-DFT calculations used the same level of theory.

For the complex in **1**, there is an important question as to the orientations of the coordinated pyridyl rings. In the only reported X-ray crystal structure for a related compound, *cis*-$[Ru^{II}(NH_3)_4(isn)_2][ClO_4]_2$,[38] these rings lie at angles of 37.2 and 38.6° with respect to the *yz* plane as defined here. Whether a similar situation also pertains in a frozen glass or solution is unclear, but some degree of rotation about the Ru−N(pyridyl) bonds is obviously to be expected. Within the restriction of a C_{2v} symmetric system, there are two extreme possibilities which involve having the coordinated rings being either coplanar and

(37) Note that in our previous communication,[9] (somewhat smaller) β_0 values for **1**−**4** were derived by using μ_{12} values which were adjusted to take into account the angles θ (ca. 20−50°) between μ_{12} and $\Delta\mu_{12}$ estimated from the Stark measurements. However, the theoretical analyses (see below) indicate that for the low-energy transitions $\Delta\mu_{12}$ lies along the *z* axis, whilst μ_{12} is perpendicular and along the *y* axis. For the high-energy transitions, $\Delta\mu_{12}$ and μ_{12} are parallel and lie along the *z* axis. The angles between μ_{12} and $\Delta\mu_{12}$ should therefore be 90° and 0° for the low- and high-energy transitions, respectively. Use of the component of μ_{12} along the $\Delta\mu_{12}$ directions in the two-state model will necessarily give a β_0 of 0 for a transition where μ_{12} is perpendicular to $\Delta\mu_{12}$, which is evidently nonsensical. Furthermore, we can find no literature precedent for using directionally adjusted μ_{12} values in the two-state approximation (see, for example: ref 3a, eqs 40 and 41 in which μ_y is used with $\Delta\mu_z$). We have therefore used the as-measured μ_{12} values here to derive β_0 values which should be viewed as replacements for those previously reported.

(38) Richardson, D. E.; Walker, D. D.; Sutton, J. E.; Hodgson, K. O.; Taube, H. *Inorg. Chem.* **1979**, *18*, 2216−2221.

Table 8. Results of B3P86/LanL2DZ and Finite Field Calculations for the Electronic Transitions of the Complex Cations in Salts **1** and **12**

cation structure	E_{max} (eV)	$\Delta\mu_{12}$ (D)	μ_{12} (D)	f_{os}	symmetry	major contributions	$\beta_{zyy}{}^{c}$ (10^{-30} esu)	$\beta_{zzz}{}^{c}$ (10^{-30} esu)
1a	2.42	14.7	5.4[a]	0.27	B_2	HOMO-1 → LUMO+1 (59%) HOMO → LUMO (37%)	72	
	2.66	14.3	3.1[b]	0.10	A_1	HOMO → LUMO+1 (56%) HOMO-1 → LUMO (31%)		17
1b	2.43	13.5	6.7[a]	0.41	B_2	HOMO → LUMO (93%)	91	
	2.77	12.9	3.7[b]	0.14	A_1	HOMO → LUMO+1 (86%)		19
1c	2.62	13.6	6.4[a]	0.40		HOMO-1 → LUMO+1 (48%) HOMO → LUMO (44%)	70	
	3.00	14.1	3.9[b]	0.17		HOMO → LUMO+1 (62%) HOMO-1 → LUMO (20%)		18
12	2.65	18.0	3.9[a]	0.15	B_2	HOMO-1 → LUMO+1 (92%) HOMO-1 → LUMO+2 (3%)	54	
	2.91	14.2	5.3[b]	0.31	A_1	HOMO → LUMO+1 (37%) HOMO-1 → LUMO (32%) HOMO-1 → LUMO+2 (8%)		36

[a] Transition dipole moment along the *y* axis. [b] Transition dipole moment along the *z* axis. [c] Obtained from FF calculations.

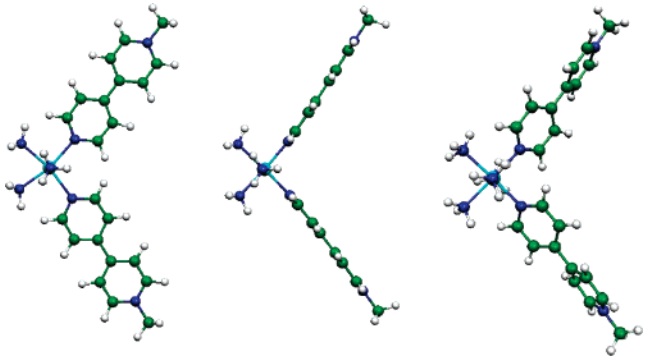

Figure 6. Conformations **1a** (left), **1b** (center) and **1c** (right) of the cation **1** used in the theoretical calculations.

lying in the *yz* plane (denoted **1a**) or both lying perpendicular to this plane (denoted **1b**). The latter option corresponds to that assumed in the earlier MO treatment of Zwickel and Creutz.[30b] In both structures, the pyridinium rings are coplanar with the adjacent pyridyl rings. To present a complete picture, we have therefore conducted calculations on both of these alternate conformations for the cation in **1**, and also for the fully optimized structure without any restrictions (denoted **1c**). The latter has an almost C_2 geometry, with the coordinated pyridyl rings lying at an angle of 45° (in the same direction) with respect to the *yz* plane, in fashion similar to that for the related crystal structure,[38] while the pyridinium rings are rotated by 77° out of the *yz* plane (again in the same direction). The three conformations of the cation in **1** are shown in Figure 6.

According to the TD-DFT calculations, the complex cation in **1** has several absorption bands below 3 eV, but only the two of these which have substantial intensity will be considered here (Table 8). The predicted E_{max} and $\Delta\mu_{12}$ values are generally somewhat larger than the corresponding experimental data (Tables 1 and 7), but no consistent pattern is observed in the μ_{12} values. More importantly, but not unexpectedly, our calculations conclude that the model previously proposed for related complex chromophores *cis*-$[Ru^{II}(NH_3)_4(L^1)_2]^{2+}$ (L^1 = py, etc.) by Zwickel and Creutz[30b] is only valid for the **1b** conformation. For conformations **1a** and **1c**, a more complex model is required since the HOMO is not the only occupied orbital involved in the low-energy electronic transitions; the HOMO−1 is very close in energy to the former and also contributes to these transitions. The molecular orbitals involved in these low-energy transitions in the complex cation in salt **1** are shown in Figure 7 (for simplicity, only the **1a** conformation is depicted). It can be seen that the HOMO and HOMO−1 are both ruthenium d orbitals, while the LUMO and LUMO+1 are π orbitals located on the 4,4′-bipyridinium ligands and consequently these transitions are MLCT processes.

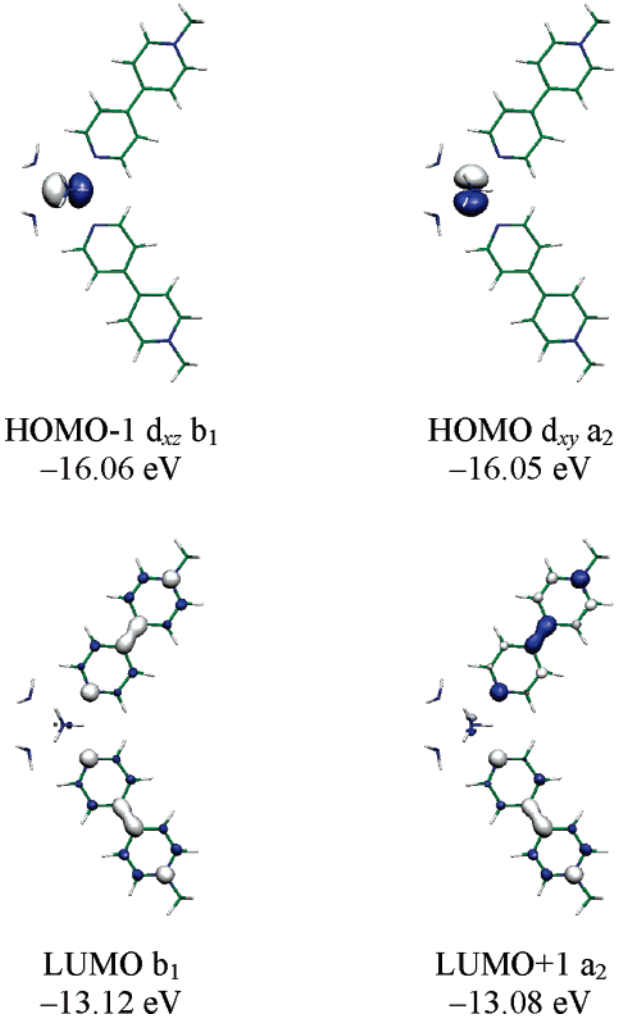

Figure 7. Illustration of the 0.06 contour surface diagrams of the molecular orbitals of **1** (conformation **1a**) involved in the two lowest-energy transitions

Although conformational changes in the cation in **1** modify the contribution of different orbitals to the MLCT transitions and hence their energies and oscillator strengths, their sym-

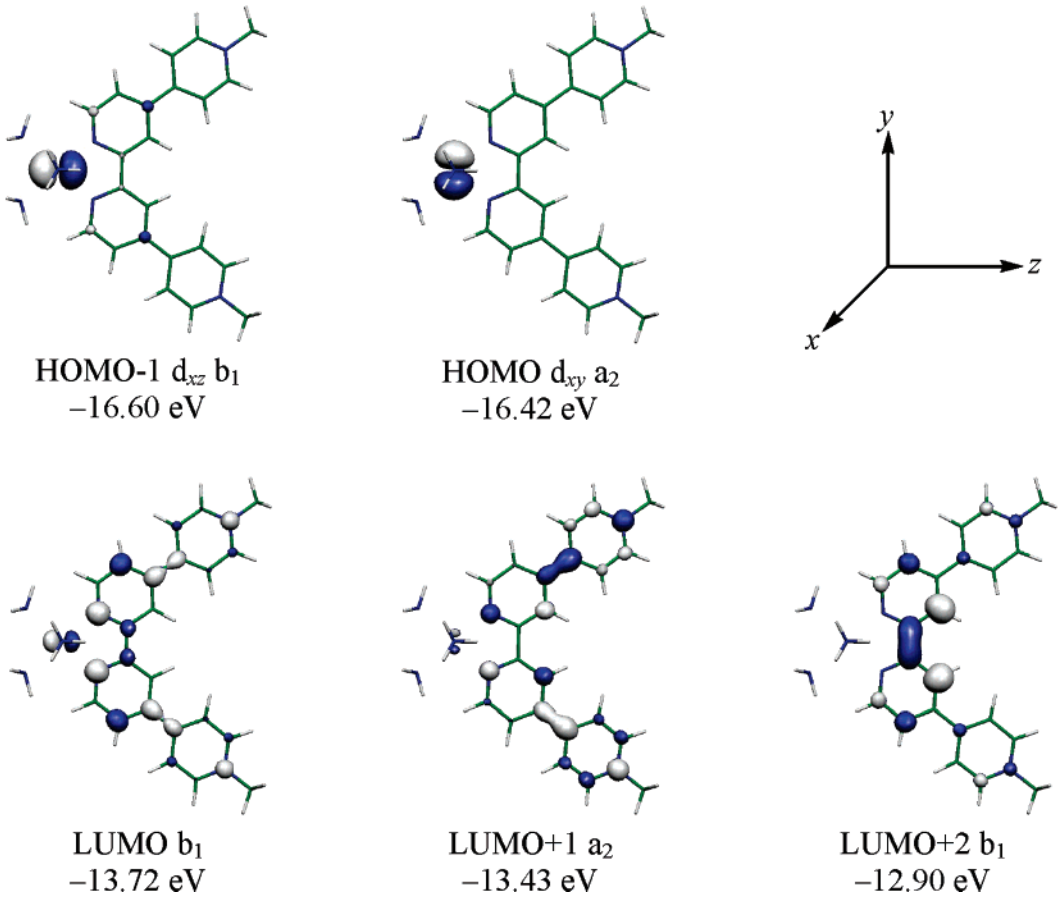

Figure 8. Illustration of the 0.06 contour surface diagrams of the molecular orbitals of **12** involved in the two lowest-energy transitions (structure restricted to having all four rings coplanar)

metries are unchanged: the lowest-energy transition is polarized along the *y* axis, while the second lowest-energy transition is polarized along the *z* axis. Considering that the dipole moments of ground and excited states are directed along the *z* axis, the lowest-energy transition should be associated with the β_{zyy} response and the higher-energy transition with β_{zzz}. The β values shown in Table 8 have been evaluated using the FF approach which involves the numerical calculation of the second derivative of the dipole moment with respect to the electric field. Quite surprisingly, β_{zzz} is nearly insensitive to the molecular conformation while β_{zyy} does not change on passing from conformation **1a** to **1c**, but reaches a somewhat higher value in conformation **1b** with the pyridyl rings perpendicular to the *yz* plane. Although these calculated β values differ somewhat from those obtained by applying eq 7 to the Stark data (Table 7), they do verify the 2D nature of the NLO responses.

Calculations on the complex cation in **12** were performed restricted to the C_{2v} symmetry[39] with all four rings lying in the *yz* plane, which can be directly compared to **1a**. The results of these calculations are shown in Table 8, and the molecular orbitals involved in the low-energy transitions are depicted in Figure 8. It should be noted that transitions to the LUMO+2 have an important contribution to the lowest-energy absorptions in the case of the cation in **12**, but not for that in **1**. This effect is due to the linking of the two 4,4′-bpy ligands in **12** that causes a lowering in the energy of the LUMO−2, which is in this instance only 0.47 eV above the LUMO, compared to 1.45 eV above the LUMO in **1**. The calculated E_{max} values show that these electronic transitions are hypsochromically shifted in **12** when compared with **1**. On moving from **1** to **12**, μ_{12} and f_{os} decrease for the lowest-energy transition and increase for the high-energy one. In any case, the symmetries of these MLCT transitions are the same in both **1** and **12**: the lowest-energy transition has B_2 symmetry, while the second lowest-energy transition is A_1. The predicted differences (which mostly parallel the experimental trends shown in Table 7) account for a decreased β_{zyy} and an increased β_{zzz} for **12** when compared with **1**, as confirmed by our FF calculations and the Stark measurements. However, the latter data indicate that β_{zzz} for **12** is actually larger than β_{zyy}, in contrast with the FF results. It is worth noting that the results of our calculations are consistent with those of previous ZINDO studies on the prototypical complex *cis*-$[Ru^{II}(NH_3)_4(2,2'\text{-bpy})]^{2+}$ which predict only relatively weak MLCT transitions polarized perpendicular to the bpy plane.[32b]

Previous ZINDO computational studies have addressed the effects on linear absorption and quadratic NLO properties of the dihedral angles between aryl rings in purely organic chromophores, as a potential approach to modulating optical behavior at the molecular level.[40] Similar studies have also been carried out with the organometallic complex *trans*-$[Ru^{II}(C{\equiv}CC_6H_4C_6H_4NO_2\text{-}4,4')Cl(dppm)_2]$ [dppm = bis(diphenylphos-

(39) A full unrestricted geometry optimization of the cation in **12** resulted in the pyridinium rings being rotated by ca. 38° with respect to the pyridyl rings. However, the properties calculated for this geometry are similar to those reported in Table 8 for the completely planar conformation: E_{max} = 2.79 and 2.88 eV.; $\beta_{zyy} = 42 \times 10^{-30}$ esu; $\beta_{zzz} = 30 \times 10^{-30}$ esu.

phino)methane].[41] It is notable that, because our FF calculated β_{zyy} values for the complex chromophore in **1** show some variation as the relative orientations of the pyridyl and pyridinium rings are changed, such species correspond (at least in theory) to systems in which the relative 2D nature of the β response can be controlled.

Further Comments on the NLO Properties of the Chromophores in 1−4. Our theoretical analyses of the cation in **1** are consistent with the observed visible absorption and Stark spectroscopic results for **1**−**4** in predicting two MLCT transitions, the lower-energy one corresponding with the larger off-diagonal β component (β_{zyy}) and the higher-energy one corresponding with the smaller β component (β_{zzz}) (Tables 7 and 8). Although the Stark data do not clearly identify which β component corresponds with each transition,[42] application of the theoretical outcomes to the Stark results gives a β_{zyy}/β_{zzz} ratio of 2−3 for **1**, **3**, and **4**, while the corresponding FF-derived ratios for the cation in **1** are ca. 4−5 for all three conformations. This observed dominance of the NLO response by off-diagonal β component(s) is very unusual and somewhat reminiscent of the purely organic chromophore *N*,*N*′-dihexyl-1,3-diamino-4,6-dinitrobenzene, for which β_{zyy} and β_{yzy} have been found to be similar and about an order of magnitude larger than β_{zzz}.[3l] However, for **1**−**4** there is clearly a discrepancy between the calculated and HRS-derived β components, because the latter data indicate that β_{zzz} is ca. 2−3 times larger than β_{zyy} (Table 6). It appears likely that this apparent discrepancy may arise from dispersion and resonance effects.

Previous polarized HRS studies by Kaatz and Shelton involving the triarylmethane dye Brilliant Green (BG)[43] are especially relevant to our studies. The C_{2v} chromophore in BG has an intramolecular charge-transfer absorption band at λ_{max} = 632 nm [in 1,4-dioxane/methanol (95:5)], and HRS measurements were carried out with both 1319 and 1064 nm lasers, giving SH wavelengths of 660 and 532 nm, on either side of the resonance peak.[43] These experiments yielded β and ρ values similar to those which we have obtained for **1**−**4**, and further ρ measurements using elliptically polarized incident light were employed to test the validity of some of the assumptions made in the analysis of the polarization results. With the SH at 660 nm, a *k* value of −0.34 was obtained for BG (very similar to that for **1**), and the assumptions of 2D β and Kleinman symmetry were found to be valid.[43] In contrast, the elliptically polarized data showed that Kleinman symmetry is broken when using the 532 nm SH, with out-of-plane β components becoming significant.[43] Subsequent HRS studies with BG and the closely related dye Malachite Green have concluded that measurements of ρ alone can give a misleading indication of the NLO character of such chromophores, if Kleinman-disallowed contributions are not taken into consideration.[3j] Similar concerns have been noted in relation to 2D Ni(II) Schiff base complexes[4f] and a Zn(II) phthalocyanine derivative.[4i]

By analogy with the published studies with BG,[43] it seems likely that a comparable situation may pertain for **1**−**4**, especially since our HRS measurements used an SH at 400 nm, on the high-energy side of the MLCT bands. Because our calculations were carried out at zero frequency where Kleinman symmetry is exact, it is not wholly unexpected that their conclusions should differ somewhat from those derived from HRS measurements at an optical frequency where Kleinman symmetry breaking may occur. The calculations indicate that the higher-energy MLCT transition, which is closer to resonance when using a 400 nm SH, is the main contributor to β_{zzz}. However, dispersion may change a measured β value by as much as an order of magnitude when compared with β_0, and the dispersion effects may be different for the β_{zzz} and β_{zyy} components because these are associated with transitions which lie at different distances from resonance.

Conclusions

We have synthesized and characterized the first family of charged 2D dipolar NLO chromophores based on redox-switchable transition metal centers. These *cis*-$\{Ru^{II}(NH_3)_4\}^{2+}$ compounds are found to display relatively large and 2D first hyperpolarizabilities by HRS at 800 nm, and Stark spectroscopic studies also show that the NLO responses have two substantial orthogonal components. The orbital structures have been elucidated by using TD-DFT which shows that the lowest-energy MLCT transition is associated with the β_{zyy} response and the higher-energy transition with β_{zzz}. The β values obtained from FF calculations are somewhat smaller than those derived from the Stark data, and β_{zyy} shows some variation as the relative orientations of the pyridyl and pyridinium rings are changed. Further studies will involve the maximization of β responses by modifications of the electron-accepting ligand structures and co-ligands. We also intend to investigate the possibilities for multistate redox-switching of the NLO properties by exploiting reversible $Ru^{III/II}$ oxidation processes and ligand-based reductions.

Acknowledgment. We thank the EPSRC for support (Grants GR/M93864 and GR/R54293) and also the Fund for Scientific Research-Flanders (FWO-V, G.0297.04), the University of Leuven (GOA/2000/3), the Belgian Government (IUAP P5/3), MCyT-FEDER (BQU2002-00219), and Gobierno de Aragon-Fondo Social Europeo (P009-2001 and E39). This research was partially carried out at Brookhaven National Laboratory under Contract No. DE-AC02-98CH10886 with the U.S. Department of Energy and supported by its Division of Chemical Sciences, Office of Basic Energy Sciences. Dr. Kurt Wostyn is thanked for his assistance with some of the HRS measurements, and we are very grateful to Profs. David P. Shelton (UNLV) and Santo Di Bella (Università di Catania) for some helpful comments regarding the physical aspects of these studies.

Supporting Information Available: Cartesian coordinates of theoretically optimized geometries for the cation conformations **1a**, **1b**, **1c** and for the cation in **12** (C_{2v} and C_1 forms); complete ref 25. This material is available free of charge via the Internet at http://pubs.acs.org.

JA0424124

(40) (a) Albert, I. D. L.; Marks, T. J.; Ratner, M. A. *J. Am. Chem. Soc.* **1997**, *119*, 3155−3156. (b) Albert, I. D. L.; Marks, T. J.; Ratner, M. A. *J. Am. Chem. Soc.* **1998**, *120*, 11174−11181.

(41) McDonagh, A. M.; Whittall, I. R.; Humphrey, M. G.; Skelton, B. W.; White, A. H. *J. Organomet. Chem.* **1996**, *519*, 229−235.

(42) Note however that the observation that the Stark-derived θ value is, in every case, considerably larger for the lower-energy transition than for the higher-energy one[9] is consistent with the assignment of the former transition as corresponding with the β_{zyy} component for which μ_{12} is perpendicular to $\Delta\mu_{12}$ (i.e. $\theta = 90°$).

(43) Kaatz, P.; Shelton, D. P. *J. Chem. Phys.* **1996**, *105*, 3918−3929.